Photonik
Ingenieurbüro
Dr. Walter Luhs

LM-0600 HeNe Laser Gyroscope

Table of Contents

1.0 Introduction

Despite the existence of high precision satellite navigation (GPS) each transport vehicle which relies on navigation must have its own GPS independent navigation system to be prepared if the GPS may fail. Regardless of the manufacturer like Airbus or Boeing, air planes nowadays are equipped with laser gyroscopes for navigation. Shortly after the invention of the laser in 1960, the idea of Georges Sagnac from 1913 (France)was applied with a HeNe ring laser.

However the difference of such a ring laser gyroscope to the idea of Sagnac lies in the fact that within Sagnac's set-up the light source is separate from the ring structure and the signal is as a phase shift between the counter propagating beams. In the laser gyroscope discussed and applied here, the light source is part of the ring laser and the output is a beat frequency between the counter propagating laser modes. This class of laser gyroscopes are termed as "active" and those of the Sagnac' s type as "passive" laser gyroscopes. In general the active laser gyroscope provides much higher precision and long term stability as the passive ones. The precision of the laser gyroscope becomes more evident, when it is compared to other well known measuring devices for instance a micrometer screw with a resolution of 0.01 mm. It must have at least a length of at least 3 km (!) for having the same resolution. Within this experimental work, the basics of the laser gyroscope are explained and practically studied at the system, which allows full access to all components. The experimental laser gyroscope consists of a rugged turntable on which the ring laser is mounted. A rotational stage, driven by a stepper motor which rotates the turntable. The angular speed and range can be set via the provided controller. The ring laser consists of three laser mirrors arranged at the corners of an equilateral triangle. The point of rotation lies well within the centre of this triangle. At one mirror a beam bending device is positioned in such a way, that the clockwise and counter clockwise propagating modes are superimposed and their beat frequency is detected by means of two photo detectors. The signal of the photodetector has a phase shift of 90° to each other so that a subsequent direction discrimination is performed. The created TTL signal is fed to a frequency counter. For the first alignment of the ring laser an adjustable green laser pointer is used. Once the system is aligned, the single mode etalon is inserted to obtain the required single mode operation. The beat frequency of the modes is measured as function of the angular speed. A special measurement is focused on the so called lock-in threshold, which is an unwanted effect of active laser gyroscopes.
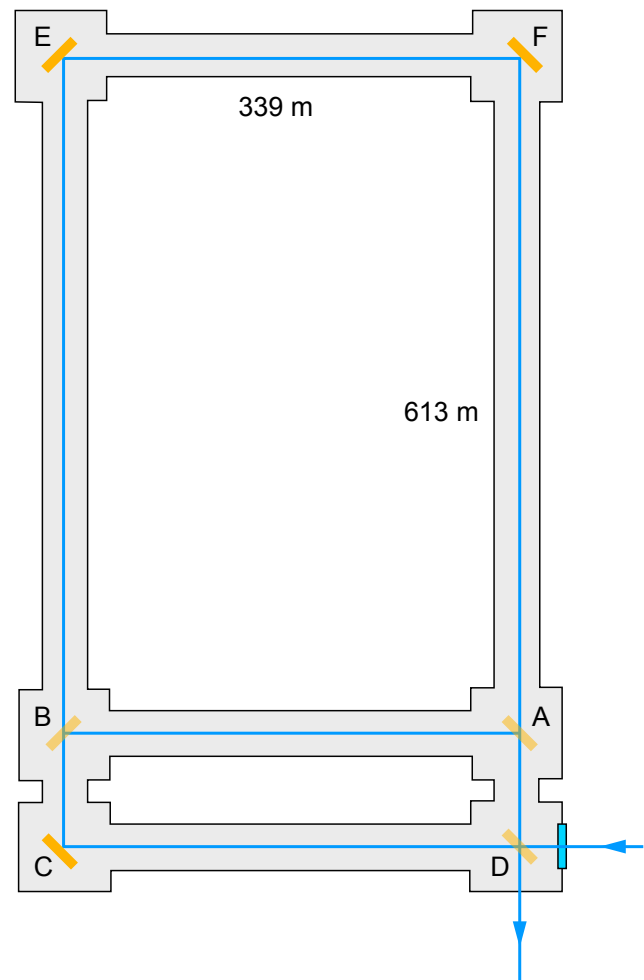

Fig. 1: Michelson Gale ring resonator experiment 1925

2.0 Fundamentals

2.1 Characteristics of light

Light, the giver of life, has always held a great fascination for human beings. It is therefore no coincidence that people have been trying to find out what light actually is for a very long time. We can see it, feel its warmth on our skin, but we cannot touch it. The ancient Greek philosophers thought light was an extremely fine kind of dust, originating in a source and covering the bodies it reached. They were convinced, that light was made up of particles. As humankind progressed and we began to understand waves and radiation, it was proved that light did not, in fact, consist of particles but that it is an electromagnetic radiation with the same characteristics as radio waves. The only difference is in the wavelength. We now know that the characteristics of light are revealed to the observer depending on how he sets up his experiment. If the experimenter sets up a demonstration apparatus for particles, he will be able to determine the characteristics of light particles. If the apparatus is one used to show the characteristics of wavelengths, he will see light as a wave. The question we would like to be answered is: What is light in actual fact? The duality of light could only be understood using modern quantum mechanics. Heisenberg showed, with his famous "uncertainty relation", that strictly speaking, it is not possible to determine the place x and the impulse p of any given occurrence at the same time

$$\Delta x \cdot \Delta p_x \geq \frac{1}{2}\hbar$$

If, for example, the experimenter chooses a set up to examine particle characteristics, he will have chosen a very small uncertainty of the impulse px. The uncertainty x will therefore have to be very large and no information will be given on the course of the occurrence. The uncertainty is not given by the measuring apparatus, but is of basic nature. This means that light always has the particular property, the experimenter wants to measure. We can find out about any characteristic of light as soon as we think of it. Fortunately the results are the same, whether we work with particles or wavelengths, thanks to Einstein and his famous formula:

$$E = m \cdot c^2 = \hbar \cdot \omega$$

This equation states, that the product of the mass m of a particle with the square of its speed c relates to its energy E. It also relates to the product of Plank's constant and its radian frequency.

In the further discussion of the fundamentals, we will use the wave representation and describe light as electromagnetic radiation. All types of this radiation, whether in the form of radio waves, X-ray waves or light waves consist of a combination of an electrical field $\vec{E}$ and a magnetic field $\vec{H}$. Both fields are bound to each other and are indivisible. Maxwell formulated this observation in one of his four equations, which describe electromagnetic fields

$$\nabla \times \vec{H} \approx \frac{\partial \vec{E}}{\partial t}$$

According to this equation, every temporal change in an electrical field is connected to a magnetic field (Fig. 2).
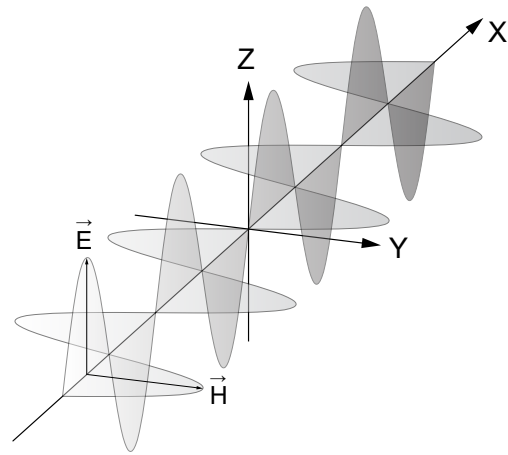

Fig. 2: Light as electromagnetic radiation

Due to the symmetry of this equation, a physical condition can be sufficiently described using either the electrical or the magnetic field. A description using the electrical field is preferred since the corresponding magnetic field can be obtained by temporal differentiation. In the experiments (as presented here) where light is used as electromagnetic radiation, it is advantageous to calculate only the electrical fields since the light intensity is:

$$I = \frac{c \cdot \varepsilon}{4\pi} \cdot \left|\vec{E}\right|^2$$

This is also the measurable property as perceived by the eye or by a detector. The speed of light is c in the respective medium and e is the corresponding dielectric constant. Since we are comparing intensities in the same medium, it is sufficient to use

$$I = \left|\vec{E}\right|^2$$
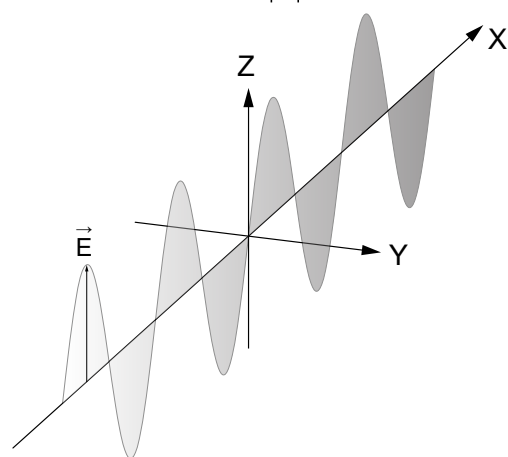
Fig. 3: In this experiment we need only consider the electrical field strength $\vec{E}$

The experimental findings agree to the theory of electromagnetic radiation (Maxwell), if the temporal behaviour of the field strength of the light $\vec{E}$ is a harmonic periodic function. In its simplest form this is a sine or cosine function. An amplitude E_0 and a wavelength λ should be used in the definition of this kind of function. Let us begin with the equation:

$$E_X = E_0 \cdot \sin\left(\frac{2 \cdot \pi}{\lambda} \cdot x\right), \qquad \textbf{(1)}$$

which we will elaborate and explain further.
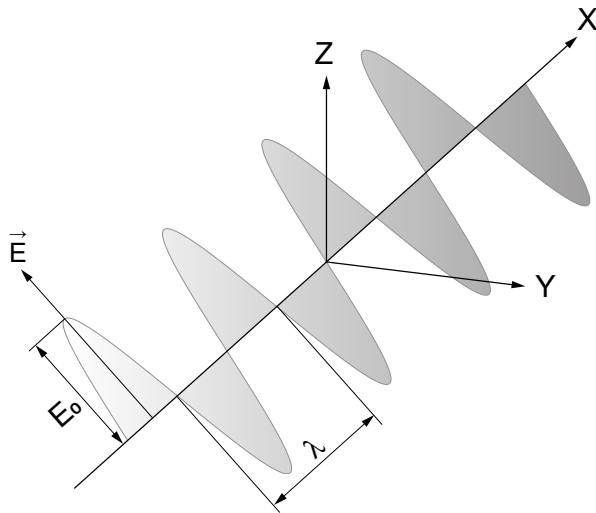
Fig. 4: Amplitude and wavelength

In the above figure the light wave no longer oscillates in the Z-direction as in Fig. 3 but at a certain angle to the Z- or Y-axis. The X-axis has been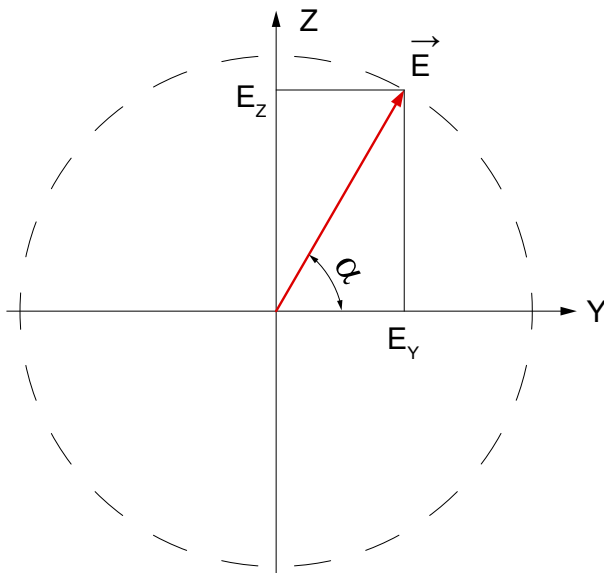 chosen as the direction of propagation of the wave. We still require information on the direction in which the electrical field strength E_x oscillates to complete the description of the wave. Strictly speaking, the field E_x oscillates vertically to the direction of propagation X. However, we have to give information regarding the Z- and Y-axis. This leads to the term 'Polarisation' and Direction of Polarisation. In Figs. 1 and 2 we used linearly polarised light with a polarisation direction in Z and in Fig. 4 we used a different direction. We will now introduce the polarisation vector P, which is defined in the following Fig. 5. We look into the light wave in the direction of the X-axis for this purpose.

Fig. 5: Definition of the polarisation vector

We observe a wave propagating in the X-direction and oscillating at the electrical field amplitude E_0 under an angle of α to the Y-axis. The amplitude E_o is separated into its components, which oscillate in the Z- or Y-direction. We now write $\vec{E}$ to indicate, that the electric field strength is now made up of individual components.

$$\vec{E} = E_x \cdot \vec{e}_x + E_x \cdot \vec{e}_y$$

In this case $\vec{e}_z = (0,1)$ and $\vec{e}_y = (0,1)$ are the unit vector in the

Z- or Y-direction in the ZY-plane. The unit vectors have the property of $|\vec{e}_z|=1$ and the scalar product $\vec{e}_y \cdot \vec{e}_z=0$. The equation (1) can be generalised to:

$$E_X(Y,Z) = \left(E_0^Y \cdot \vec{e}_y + E_0^Z \cdot \vec{e}_z \right) \cdot \sin\left(\frac{2\pi}{\lambda} \cdot x \right)$$

At this point we come across a fundamental principle in classic wave theory, i.e. the principle of superimposition. A big word for the simple statement:

Every wave can be represented as the sum of individual waves.

In our example we had separated the wave as shown in Fig.4 into two individual waves, i.e. one that oscillates in the Z-direction and another in the Y-direction. We could just as well say, that the wave is created by the superimposition of these two individual waves. The word ***interference*** can also be used to mean superimposition. In this context the wave is formed by the interference of two individual waves. that could be measured immediately with their equipment. We are using this definition, because it simplifies the written work.

2.2 Superimposition, phase and beat frequency
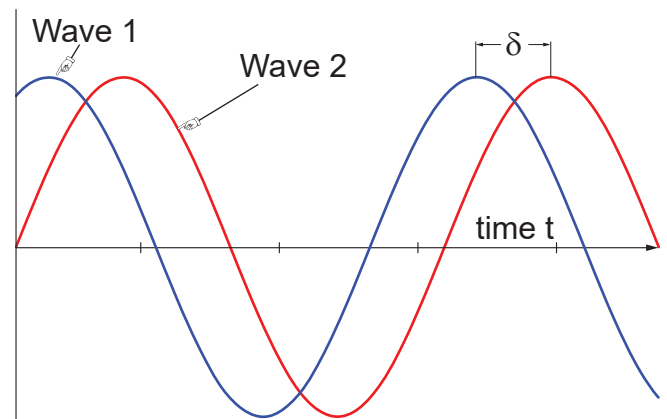
Fig. 6: Two waves with same frequency, but with a phase shift between each other

Obviously the phase δ contains information about the relationship between two or more waves. Let us presume that the waves originate in a light source and phase δ contains information on how the wave was formed. Light waves are created by emission processes and there is an emission procedure for every photon or light wave. The emission procedures are distributed statistically according to the type of the light source. Thus, the frequency or phase δ is also distributed statistically. If the emission procedures are coupled to each other, as is the case with lasers, and all photons or waves have the same frequency or wavelength such light is termed as coherent (holding itself together).

If, however, phase δ is randomly distributed, then this light is incoherent. This is the case with thermal light sources, e.g. light bulbs. According to Fig. 6 the wave 2 has a phase shift of δ as opposed to the wave 1. If we produced two such waves (this is exactly what the Michelson interferometer does), we expect a third wave through the principle of superimposition, which is formed by the superimposition or interference of the two basic waves. We will find out how this wave looks like by simply adding both basic waves:

Wave 1 $\quad \vec{E}_1 = (E_Y, E_Z) \cdot \sin(k \cdot x + \omega \cdot t + \delta)$

Wave 2 $\quad \vec{E}_2(Y,Z) = (E_Y, E_Z) \cdot \sin(k \cdot x + \omega \cdot t)$

Wave(1,2) $\quad \vec{E}_3 = \vec{E}_1 + \vec{E}_2$

A large number of waves with different frequencies ω or wavelengths λ and phases δ result in such a confusing mixture and it has no practical sense to carry out superimposition or interference experiments with such light. Therefore, light sources which emit light within a narrow emission spectrum with a phase as constant as possible are selected. Lasers are an example of such light sources.

But when Michelson carried out his experiments around 1870 he had no lasers. He used instead the red atomic emission line of a cadmium lamp whose emission bandwidth has a coherence length of only 20 cm requiring sophisticated experimental arrangements.
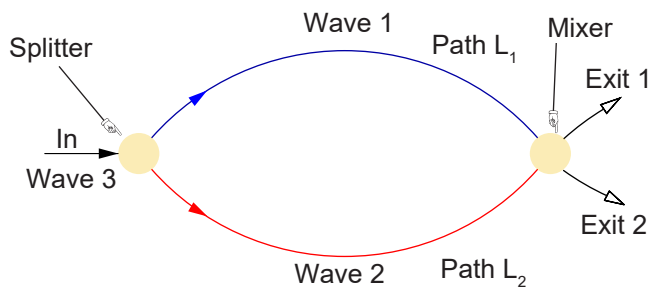
Fig. 7: **Generalized treatment of interference**

We will discuss basic devices to superimpose light waves like the Michelson interferometer. A generalized approach is shown in Fig. 7. Each interferometer uses a light source (Wave 3), which radiation is split into two portions of equal intensity. An ideal splitter would not affect neither the wavelength nor the phase of the created waves. Wave 1 and wave 2 are travelling along individual paths and are combined in the mixer. It should be noted, that each interferometer has at least two exit paths, which is required to fulfil the energy conservation. As we will see later that in case of a destructive interference at exit 1 the energy is not destroyed, but it leaves the interferometer at exit 2.

The idea of the formalism is to create two waves, wave 1 and wave 2 and calculate their superimposition at exit 1 or exit 2.
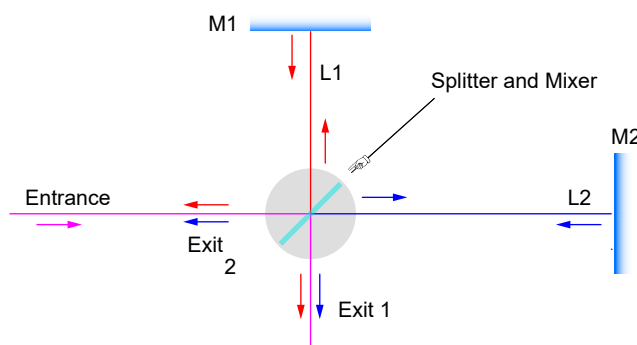
Fig. 8: **The famous Michelson interferometer**

Such an arrangement is shown in Fig. 8, the famous Michelson interferometer. In this setup the splitter and mixer are identical.
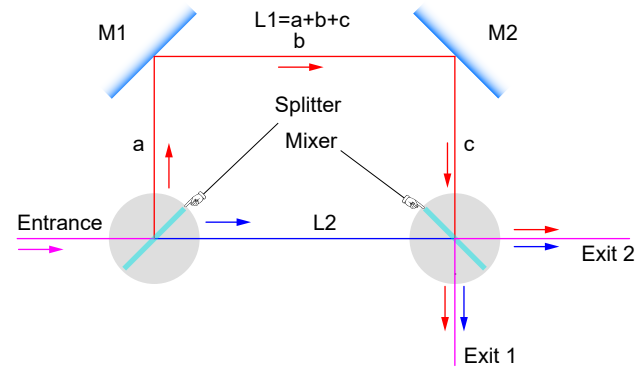
Fig. 9: **Mach Zehnder interferometer with separate splitter and mixer**

Both interferometers are belonging to the class of two-beam interferometer. A famous example of multi-beam interferometer is the Fabry Perot interferometer. However, we will not treat it here (see [1]).

Since in practical interferometer the superimposing beams travel collinear to one another we can simplify the equations and writing now:

Wave 1 $\qquad E_1 = E_{01} \cdot \sin(k \cdot L_1 + \omega \cdot t)$

Wave 2 $\qquad E_2 = E_{02} \cdot \sin(k \cdot L_2 + \omega \cdot t)$

Wave 3 $\qquad E_3 = E_1 + E_2$

Note, there is no phase shift between wave 1 and wave 2 because they are created from wave 3 and the splitter does not create an extra phase shift.

$$E_3 = E_{01} \cdot \sin(k \cdot L_1 + \omega \cdot t) + E_{02} \cdot \sin(k \cdot L_2 + \omega \cdot t)$$

Let us install a screen or photodetector at exit 1 to observe the resulting intensities. The human eye as well as photodetector cannot register pure electric fields, but can only register the light intensity I which is connected to the field strength:

$$I = E^2 = (E_1 + E_2)^2$$

$$I = (E_1 \cdot \sin(k \cdot L_1 + \omega \cdot t) + E_2 \cdot \sin(k \cdot L_2 + \omega \cdot t))^2$$
$$I = E_1^2 \cdot \sin^2(kL_1 + \omega t)$$
$$+ 2E_1 E_2 \cdot \sin(kL_1 + \omega t) \cdot \sin(kL_2 + \omega t)$$
$$+ E_2^2 \cdot \sin^2(kL_2 + \omega t)$$

By using the well known addition theorem

$$2 \cdot \sin\alpha \cdot \sin\beta = \cos(\alpha - \beta) + \cos(\alpha + \beta)$$

we get:

$$I = E_1^2 \cdot \sin^2(kL_1 + \omega t)$$
$$+ E_1 E_2 \cos(k(L_1 - L_2))$$
$$+ E_1 E_2 \cos(k(L_1 + L_2) + 2\omega t)$$
$$+ E_2^2 \cdot \sin^2(kL_2 + \omega t)$$

The fastest photodetector nowadays can follow frequencies

Theory

of up to approx. 1×10^9 Hz (1 GHZ). This is why a detector, and even more so, our eyes can only perceive slow varying average values. The $\sin^2$ terms oscillate between 0 and 1; its temporal average value is therefore 1/2. The cosine term oscillates between -1 and +1, the average value is zero, simplifying the equation to:

$$I = \frac{1}{2}E_1^2 + \frac{1}{2}E_2^2 + E_1 E_2 \cos(k \cdot \Delta L) \qquad \textbf{(2)}$$

with $\Delta L = L_1 - L_2$.

Obviously the intensity I becomes maximal when the cosine value becomes 1. This is always the case when its argument is zero or a multiple of 2π. The intensity I becomes minimal when the value of the cosine is –1 which is the case when its argument is a multiple of π.

$$I_{max} = \frac{1}{2}E_1^2 + \frac{1}{2}E_2^2 + E_1 E_2 = \frac{1}{2}\left(E_1 + E_2\right)^2$$

$$I_{min} = \frac{1}{2}E_1^2 + \frac{1}{2}E_2^2 - E_1 E_2 = \frac{1}{2}\left(E_1 - E_2\right)^2$$

Let us recall that the wave number k is defined as:

$$k = \frac{2\pi}{\lambda}$$

and that it is constant for a given wavelength. Thus, the light intensity I of eq. (2) depends only on the path difference $\Delta L = L_1 - L_2$. If the paths having the same length, both partial waves superimpose constructively and the light intensity becomes maximal. If the path difference however, is just $\lambda/2$ then the wave number k becomes:

$$k \cdot \Delta L = \frac{2\pi}{\lambda} \cdot \frac{\lambda}{2} = \pi \quad ,$$

and the value of the cosine is -1 and the light intensity I becomes minimal. If E_1 and E_2 having the same intensity, the light intensity I even becomes zero, both waves superimpose destructively.
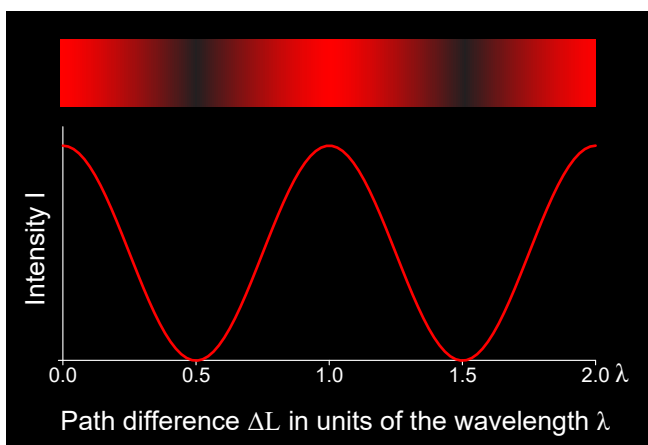

Fig. 10: Interferogram as per eq. (2)

Observing for instance a number of N dark / bright transitions, a length difference of $\Delta L = N \cdot \lambda/2$ occurred. Keeping in minds, that the wavelength used in our experiments is 633 nm, a light to a dark transition already occurs with a phase shift by only

$\lambda/2 = 316.5$ nm = 0.000000316 mm (!).

This type of interferometer is a highly precise apparatus for measuring length.

With the information of the preceding chapter, we are now prepared to approach the main topic of this project, the laser gyroscope.

2.3 Sagnac effect

The basic idea of a ring interferometer came from Georges Sagnac. The ambitions of his interest, however, was not focused on technical applications, but instead served as test of the theory of relativity of Einstein (1910 – 1920). During that time, the relativity principle of electrodynamics referred exclusively to translation movements. However, it was already known from the mechanics, processes behave differently in a rotating system than in a non-rotating system. This is shown, for example, by the pendulum experiment of Foucault, which has proven the rotation of the earth. The equations of motion of rotating mechanical systems were amended as a result to apparent forces like the centrifugal and the Coriolis force were integrated. Harress (1912) and then Sagnac (1913) studied the question of how electromagnetic radiation like light would behave in a rotating system. We shall discuss here first the results of Sagnac, since the later developed laser gyroscope was based on them.
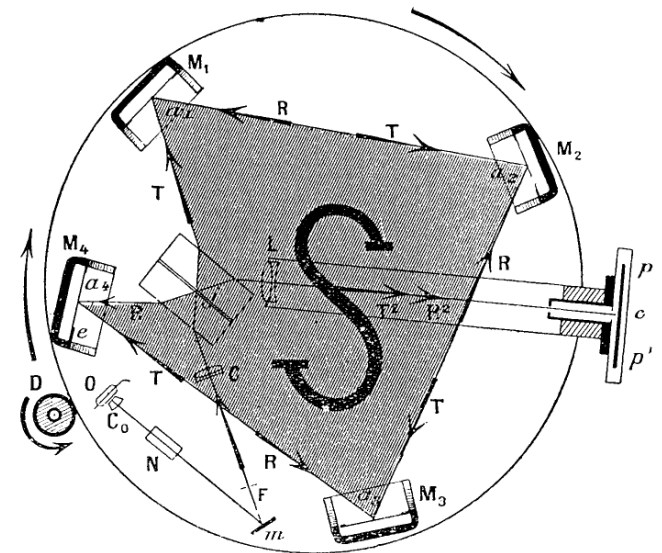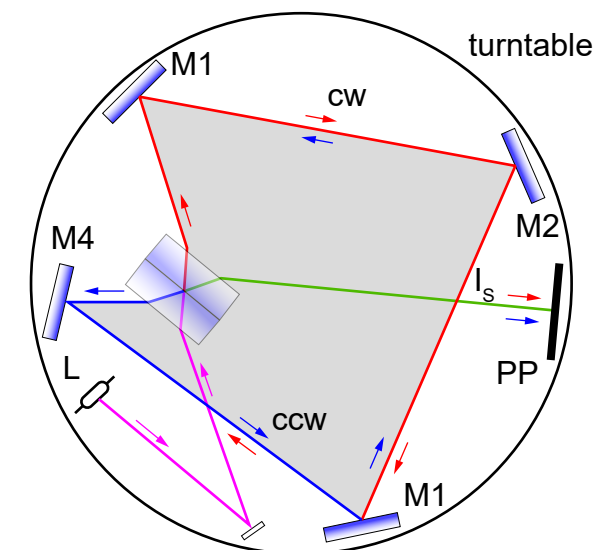

Fig. 11: Sagnac's original sketch

Fig. 12: Redrawn for more clarity

The Fig. 11 shows the original sketch of Sagnac's interferometer. He used the atomic emission of a mercury lamp (L).

Theory

Such a lamp emits even more lines, which are not useful for these experiments and must be blocked by a variety of filters. Furthermore additional optics is required to obtain almost parallel beams. The lamp as well the photographic plate (PP) is attached to the turntable. A beam splitter cube is used to split the incoming light into a cw and ccw beam. Both beams are combined again by the same beam splitter after passing one round trip. A telescope is used to image the interfering cw and ccw beams onto a photographic plate. The greyed out area indicates the area A, which is encompassed by the propagating cw and ccw beams.

The phase shift Δφ of the interference fringes is proportional to the turntable's angular velocity ω and is given by a formula originally derived by Sagnac:

$$\Delta\phi = \frac{8\cdot\pi}{\lambda\cdot c}\cdot\omega\cdot A,$$

where A is the oriented area of the loop and λ the wavelength of light.

The rotation thus measured, is an absolute rotation, that is, the turntable's rotation with respect to an inertial reference frame.

We shall now derive Sagnac's formula. For this we presume, that the turntable is rotating in counter-clockwise (ccw) direction with an angular speed of ω. The first task is to determine the velocity v for all the elements ds of the path of the light rays and then to determine their run-time difference ΔT.

$$\Delta T = T_- - T_+ = \oint\frac{ds}{v_-(ds)} - \oint\frac{ds}{v_+(ds)} \qquad (3)$$

The number *N* of the bright / bright transitions is calculated in the same way as in Michelson interferometer:

$$N = \Delta T\cdot\nu = \Delta T\cdot\frac{c}{\lambda} \qquad (4)$$

Whereby c is the speed, $\nu = c/\lambda$ the frequency and λ the wavelength of the light waves.
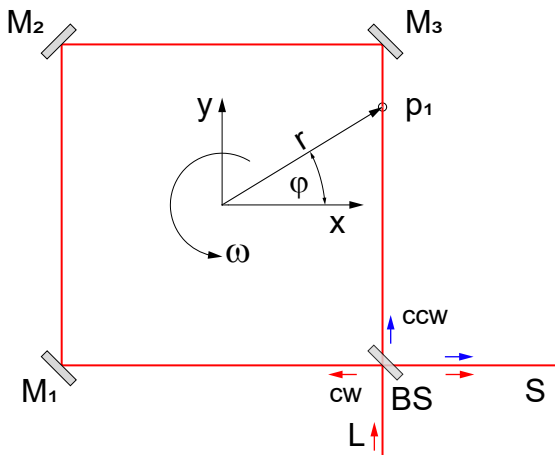

Fig. 13: Generalized Sagnac interferometer

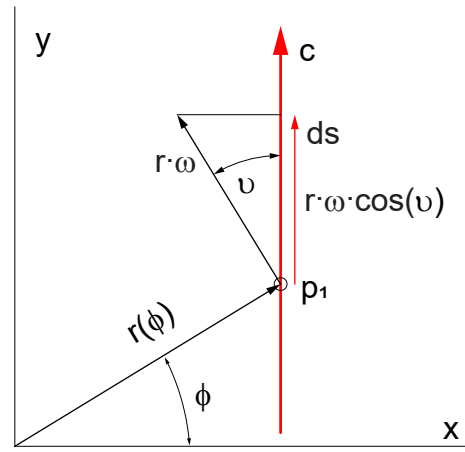**Fig. 14: Determination of the speed of the wave at point p₁**

We shall first consider the speed of the wave at the point p₁ in the direction of rotation v_+. The linear velocity v here, at a distance r from the centre of rotation, is:

$$v = r\cdot\omega$$

However, for the linear element ds in the direction of the wave with speed c, it is:

$$v = r\cdot\omega\cdot\cos\upsilon$$

This gives the total speed of the wave for the linear element ds as:
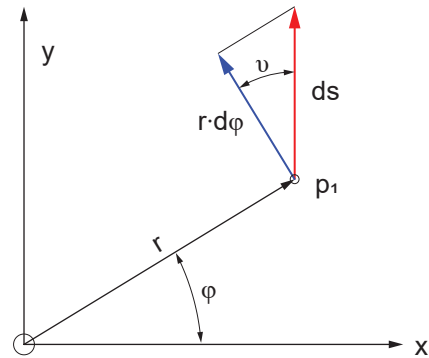
$$v_+ = c + r\cdot\omega\cdot\cos\upsilon$$

Fig. 15: Determining cos (υ)

The point p₁ moves with a velocity of r·dφ and from Fig. 15, we can conclude:

$$\cos\upsilon = \frac{r\cdot d\phi}{ds}.$$

The equation eq. (3) thus becomes:

$$\Delta T = \oint\frac{ds}{c - r^2\cdot\omega\dfrac{d\phi}{ds}} - \oint\frac{ds}{c + r^2\cdot\omega\dfrac{d\phi}{ds}}$$

or

$$\Delta T = \frac{2\omega}{c^2}\oint\frac{r^2 d\phi}{1 - \left(r^2\cdot\dfrac{\omega}{c}\cdot\dfrac{d\phi}{ds}\right)^2}$$

since $\dfrac{\omega}{c} << c$ the above equation is simplified to:

$$\Delta T = \frac{2\omega}{c^2} \oint r^2 d\phi = \frac{4A}{c^2} \cdot \omega \quad,$$

and with:

$$\frac{\Delta\varphi}{2\pi} = \frac{\Delta s}{\lambda} = \frac{c}{\lambda} \cdot \Delta T \Rightarrow \Delta\varphi = \frac{2\pi c}{\lambda} \cdot \Delta T$$

we get the equation as derived already from Sagnac:

$$\Delta\varphi = \frac{2\pi c}{\lambda} \cdot \frac{4A}{c^2} \cdot \omega = \frac{8\pi}{\lambda c} \cdot A \cdot \omega \qquad \textbf{(5)}$$

The phase shift of fringes is thus proportional to the angular speed ω and the area A, which is encompassed by the path of the light rays. The displacement of the interference pattern has been actually observed by Sagnac in one of his experiments, where he used a rotating platform with a diameter of 1 metre. In other experiments he used much longer light paths on board of a ship which was driving narrow curves to obtain the angular speed. Sagnac believed, that his experiment proved the existence of the aether, against Einstein's theory and the Michelson Morley experiment. For this reason Michelson and Gale (1925) took up the fight and built a huge ring interferometer using the rotation of the earth itself to verify the effect.
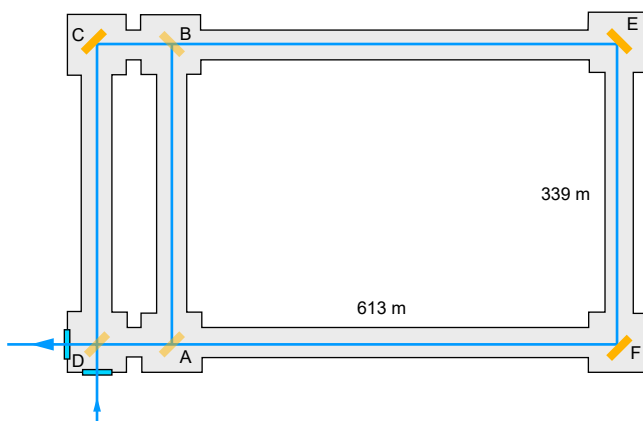

Fig. 16: Michelson Gale ring interferometer with a 1.9 km long perimeter

Fig. 17: The Michelson Gale Experiment has been performed in Clearing, Illinois

"Well, gentlemen, we will undertake this, although my conviction is strong that we shall prove only that the earth rotates on its axis, a conclusion which I think we may be said to be sure of already."

These can be considered as some excellent achievements of engineering if one considers the conditions at that time, when such a coherent source of light as a laser was still not available. Even Einstein was awed by the achievement of Michelson and Gale, who with the help of his ingenious construction, were able to prove the rotation of Earth and did not become a victim of mirror adjustments or other dirt effects. About 70 years after the works of Michelson, scientists at the University of Canterbury again constructed an interferometer, to measure the rotation of the earth.
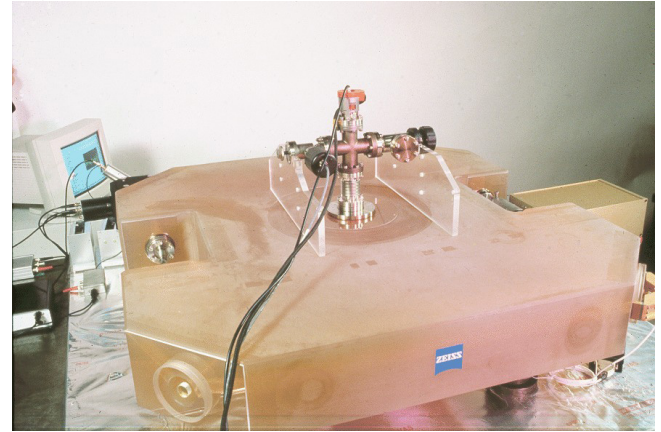

Fig. 18: CII Interferometer, which is now equipped with a laser and a Zerodur block

The so-called CII Interferometer, which is now equipped with a laser and has been made out of a Zerodur block to ensure a long-term stability. It is located in a bunker in the Cashmere Cavern (New Zealand). Together with many institutions, the questions about the constancy of the rotation of earth and the theory of relativity are being worked out here. In the next section, the structure of the interferometers being used nowadays that use the Sagnac effect for measuring rotations is introduced.

Theory

2.4 Active ring resonator

The interferometer described by Sagnac and Michelson consists out of a mirror ring structure, whereby the light source was located outside the interferometer (see Fig. 11 and Fig. 16).

Right after the invention of the Helium Neon laser (A. Javan, 1960) the idea of a ring laser gyroscope was born by Rosenthal [3] in 1961.
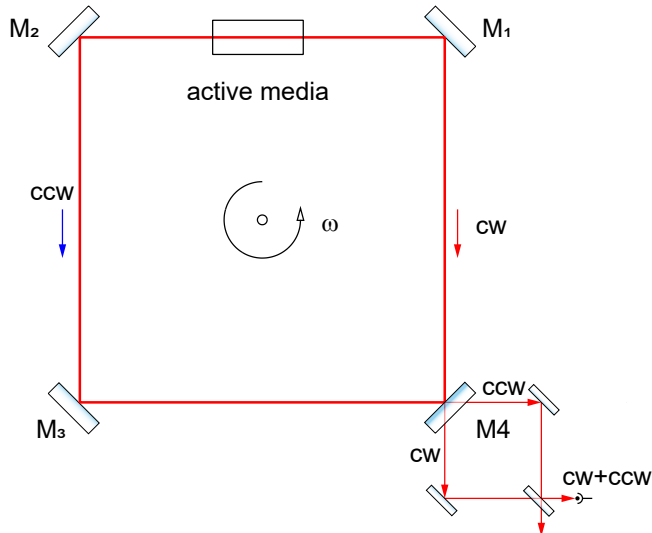

Fig. 19: Active ring laser as proposed by A. H. Rosenthal [3] in 1961

Rosenthal's idea took just another two years before a suitable setup could practically demonstrated by Macek [4] et. al. He used 4 Helium Neon tubes sealed with Brewster windows in a 1 m square arrangement. The ring laser was operated at the invisible 1.153 μm line, giving even more complication with the alignment. Macek worked for the Sperry Gyroscope Company in New York and the goal of this research was clearly targeting navigational systems for missiles and air crafts.

A variety of companies invested in this new research area and from about 1970 the first commercial ring laser gyroscopes (RLG) made by Honeywell entered the market [5].

Meanwhile the RLG became an indispensable navigation tool for aeroplanes, vessels and all earthbound systems requiring precise navigation. Surprisingly still the used laser source is a Helium Neon laser, which we will discuss briefly in the next chapter.

## 2.5 Helium Neon (HeNe) Laser
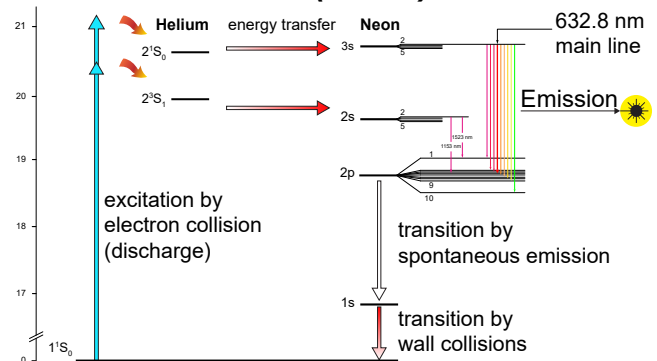
Fig. 20: HeNe laser energy level diagram

To achieve laser operation it is required to create and maintain a population inversion between two energy level. For Neon (Ne), these are the 3s, 2s as upper and the 2p energy level as lower lying state. To create the inversion, Helium is used as helper to populate the 3s and 2s states of Ne. The Helium itself is excited by an electrical discharge, which populates its metastable 2^1S_0 and 2^3S_1 states. The only way to get the Helium atoms de-excited may happen by the collisions of the excited He atoms with Ne atoms of the ground state. Consequently the Ne atoms are excited into their 3s and 2s states, whereby the 2p remains unaffected and the desired population inversion is created. To maintain the population inversion, the 2p state needs to be emptied. In a first step this happens via the transition by spontaneous emission 2p→1s. Unfortunately the 1s is a metastable state and optical emission from here to the ground state are not allowed. The only way to remove this bottle neck in the laser cycle is due to the wall collisions, this is why modern HeNe laser tubes are using capillaries through which the laser beam propagates.
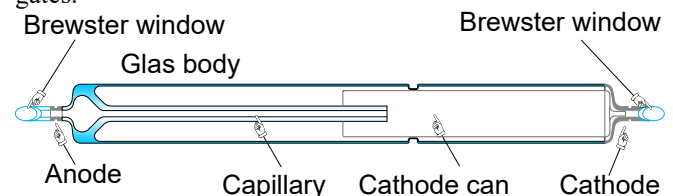
Fig. 21: Modern HeNe laser tube with Brewster windows
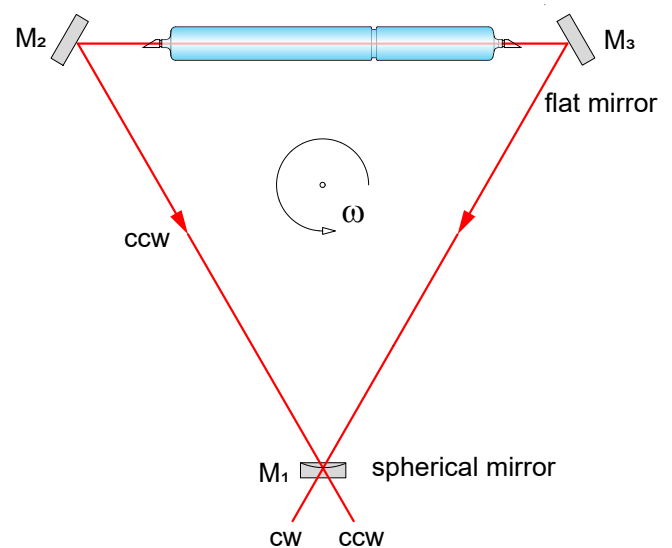

Fig. 22: HeNe Ring laser gyroscope

The Fig. 22 shows a ring laser gyroscope using a Helium

Neon laser with Brewster windows. The mirror M_2 and M_3 are flat mirrors, while M_1 is a curved one. This has an important reason. Of course one could also used three flat mirrors, but it is very hard to keep the laser beam within the cavity keeping in mind that the number of round trips is several thousands, the alignment and the flatness and surface quality of the mirror must be extremely high. This problem is eliminated, when at least one curved mirror is used which redirects escaping photons of the laser beam inside the cavity and reduces the losses tremendously, but the question is, what is the ideal radius of curvature? To answer this, we have to have a look to the stability criteria of optical resonators.

2.6 Optical Stability
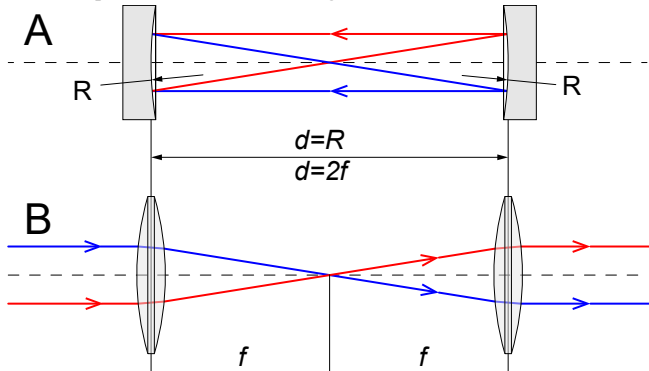
Fig. 23: Start with a two mirror cavity (A. linear cavity). B is the lens equivalent wave guide

If after endless passes the ray diameter remains smaller than the mirror diameter, then an optical resonator is called stable. In the Fig. 23 B the equivalent lens guide system is shown. The lenses need to be arranged in such a way that the rays of the left side (input) have the same properties on the right side (output). These calculations can be very cumbersome, especially when more mirrors (lenses) involved. Kogelnik and Li [6] introduced the ABCD matrix formalism, an elegant method to calculate the stability criterion for an optical resonator. We will follow some steps presented by the authors in their publication [6].
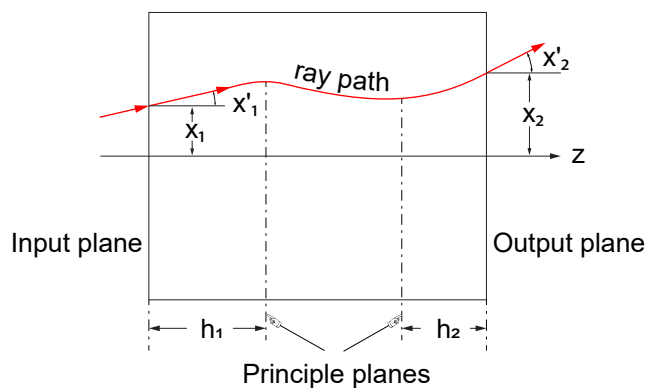
Fig. 24: Ray path in an optical system with the reference planes

A paraxial (parallel to the optical axis) ray in a given cross section (z=const) of an optical system is characterized by its distance x from the optic (z) axis and by its angle or slope x' with respect to that axis. A typical ray path through an optical structure is shown in Fig. 24. The slope x' of paraxial rays is assumed to be small. The ray path through a given structure depends on the optical properties of the structure

and on the input conditions, i.e., the position x and the slope x' of the ray in the input plane of the system. For paraxial rays the corresponding output quantities x_2 and x_2' are linearly dependent on the input quantities. This is conveniently written in the matrix form

$$\begin{vmatrix} x_2 \\ x_2' \end{vmatrix} = \begin{vmatrix} A & B \\ C & D \end{vmatrix} \cdot \begin{vmatrix} x_1 \\ x_1' \end{vmatrix}$$

The ABCD matrix is called the ray transfer matrix. Its determinant is generally unity (AD-BC = 1).

1		$\begin{vmatrix} 1 & d \\ 0 & 1 \end{vmatrix}$	Ray transfer over distance d
2		$\begin{vmatrix} 1 & 0 \\ -\dfrac{1}{f} & 1 \end{vmatrix}$	Thin lens with focal length f
3		$\begin{vmatrix} 1 & d \\ -\dfrac{1}{f} & 1-\dfrac{d}{f} \end{vmatrix}$	Combination of 1 and 2
4		$\begin{vmatrix} 1-\dfrac{d_2}{f_1} & d_1+d_2-\dfrac{d_1 d_2}{f_1} \\ -\dfrac{1}{f_1}-\dfrac{1}{f_2}+\dfrac{d_2}{f_1 f_2} & 1-\dfrac{d_1}{f_1}-\dfrac{d_2}{f_2}-\dfrac{d_1}{f_2}+\dfrac{d_1 d_2}{f_1 f_2} \end{vmatrix}$	Two thin lenses with focal length f_1 and f_2

Table 1: Example of ray transfer matrices

Light rays that bounce back and forth between the 2 spherical mirrors of a laser resonator (Fig. 23 A) experience a periodic focusing action. The effect on the rays is the same as in a periodic sequence of lenses (Fig. 23 B) which can be used as an optical transmission line. A single element of the sequence is characterized by its ABCD matrix. The ray transfer through n consecutive elements of the sequence is described by the nth power of this matrix. This can be evaluated by means of Sylvester's theorem

$$\begin{vmatrix} A & B \\ C & D \end{vmatrix}^n = \frac{1}{\sin \Theta}$$

$$\cdot \begin{vmatrix} A \cdot \sin n\Theta - \sin(n-1)\Theta & B \cdot \sin n\Theta \\ C \cdot \sin n\Theta & D \cdot \sin n\Theta - \sin(n-1)\Theta \end{vmatrix}$$

where

$$\cos \Theta = \frac{1}{2}(A+D)$$

Theory

Periodic sequences can be classified as either stable or unstable. Sequences are stable when the trace (A+D) obeys the inequality

$$-1 < \frac{1}{2}(A+D) < 1 \qquad (6)$$

The ABCD matrix of such an element like our optical resonator of Fig. 23 is given in No. 4 of Table 1. From this, one can obtain the trace, and write the stability condition as:

$$0 < \left(1 - \frac{d}{R_1}\right) \cdot \left(1 - \frac{d}{R_2}\right) < 1$$

If we are choosing R_1 equal R_2 the stability condition becomes

$$0 < \left(1 - \frac{d}{R}\right)^2 < 1$$

and is fulfilled for all $d \le R$.

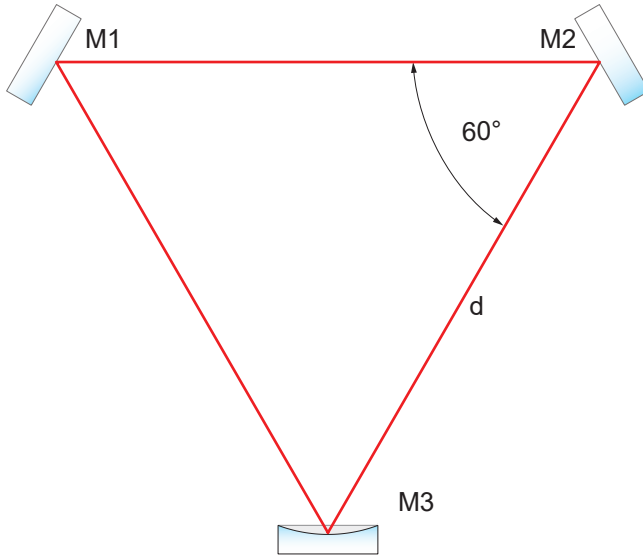In the next step, the stability condition for a 3 mirror ring laser shall be derived.

Fig. 25: Three mirror ring resonator

The mirror M_1 and M_2 are flat mirrors and M_3 is a curved one with a radius of curvature R.
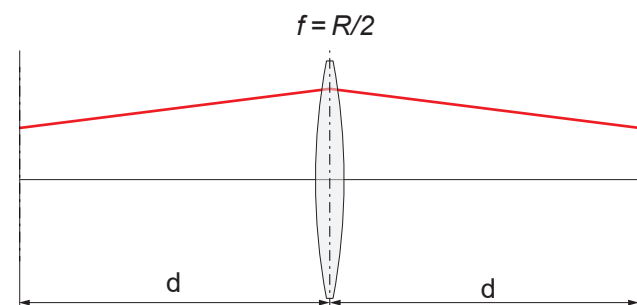

Fig. 26: Lens guide of the ring resonator of Fig. 25

The equivalent lens guide consists of three stages (from left to right):

1) Free ray path d
2) Passage though a thin lens $f=R/2$
3) Free ray path d

The related ray transfer matrix thus becomes:

$$R_T = \begin{pmatrix} 1 & d \\ 0 & 1 \end{pmatrix} \cdot \begin{pmatrix} 1 & 0 \\ -\frac{1}{f} & 1 \end{pmatrix} \cdot \begin{pmatrix} 1 & d \\ 0 & 1 \end{pmatrix}$$

$$R_T = \begin{pmatrix} 1 - \dfrac{d}{f} & d\left(2 - \dfrac{d}{f}\right) \\ -\dfrac{1}{f} & 1 - \dfrac{d}{f} \end{pmatrix}$$

The stability condition (eq. (6)) requires:

$$\frac{|A+D|}{2} = \left|1 - \frac{d}{f}\right| = \left|1 - \frac{2d}{R}\right| \le 1$$

Obviously, the three mirror ring resonator is optically stable, when the distance d fulfils the following condition:

$$\frac{R}{2} \le d \le R$$

Now we are able to create an empty optical stable ring resonator and within the next considerations we will discuss the resonator properties and in the final step we add the active material to the resonator.
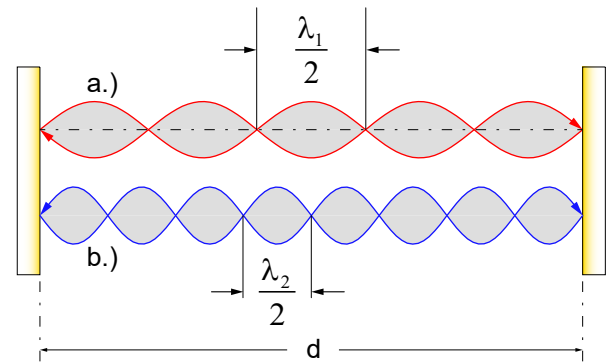
2.7 Resonator modes

**Fig. 27: Two mirror resonator with two different "resonant" modes**

The Fig. 27 shows standing waves in a resonator with a spacing of the two mirrors d. The upper curve (a.) has 6 nodes and the lower one (b.) even 9 nodes. In principle, each wave fits into the resonator, when a half of its wavelength λ is a multiple integer n of d:

$$n \cdot \frac{\lambda}{2} = d \quad \text{or} \quad n \cdot \frac{c}{2\nu} = d \quad \text{with} \quad \nu = \frac{c}{\lambda},$$

where c is the speed of light and ν its frequency.

An important parameter of a resonator or cavity is free spectral range $\Delta\nu$. That is the range where within no frequencies or modes exist. We calculate the difference of a mode with n nodes and the next neighbouring one with n+1 nodes:

$$\Delta\nu = \nu(n+1) - \nu(n) = (n+1) \cdot \frac{c}{2d} - n \cdot \frac{c}{2d} = \frac{c}{2d}$$
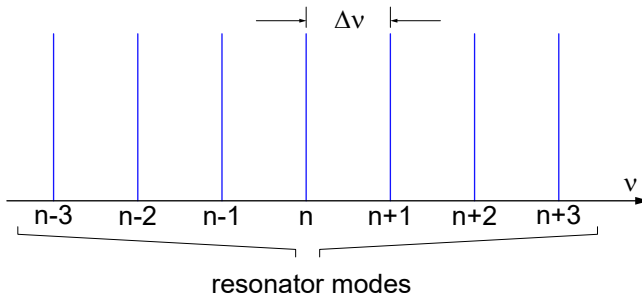
Fig. 28: The modes of a resonator

In principle a resonator can have infinitive modes, which, in turn require appropriate mirrors, which is virtually impossible. This also not required, since a laser has a comparable small gain bandwidth. This we will discuss in the upcoming section.

2.8 The active laser material

As already introduced we are using as laser material Helium Neon gas. From Fig. 20 we know that the laser transition 3p→3s is used. The 3p level is excited in such a way, that a population inversion is created, leading to the desired amplification. The combination of the active laser material and optical resonator forms the actual laser.
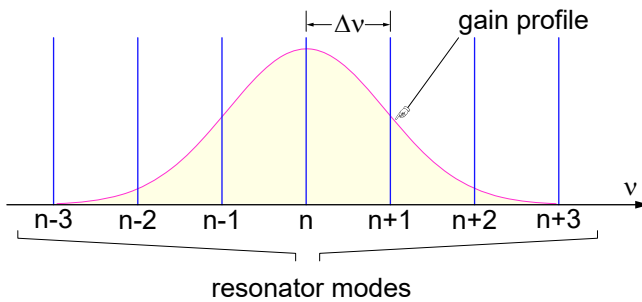
Fig. 29: Resonator with laser material

If such a cavity is filled by amplifying Neon atoms, as shown in Fig. 29, a couple of modes fit under the Neon gain profile. When the gain exceeds the losses, laser oscillation occurs. It becomes apparent that for some modes, the oscillation condition can be fulfilled resulting in a laser beam which consists out of different frequencies (or modes). For the ring laser gyroscope only a single laser frequency should exist. This could be achieved by two means, first the length of the laser cavity L is reduced and thus the distance of the modes is increased in such a way, that only one mode exists under the gain profile. However, this method also reduces the length of the amplifying medium, resulting in lower available laser power.
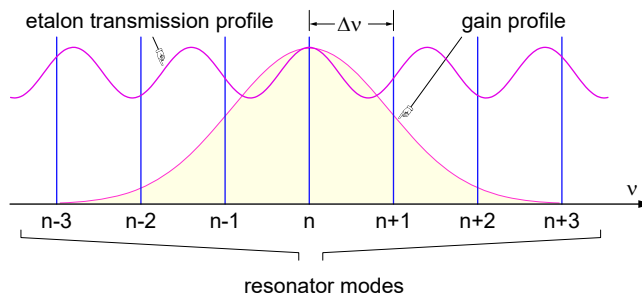
Fig. 30: Cavity with inserted etalon

Another method is the use of a so called etalon. This is a precisely ground and polished glass cylinder with extremely

parallel (<10") end faces. It forms a Fabry Perot, however the end faces are not coated, however, the 4% reflectivity (Fresnel reflection) provides a certain filter function and adds spectral losses. The transmission profile depends on the length and reflectivity of the etalon. Fig. 30 shows the combination of the laser cavity and the etalon. If the transmission maxima is tuned to the central mode, the neighbouring modes are ceasing due to the losses of the etalon and single mode oscillation is achieved. This is actually what we need for the ring laser gyroscope, which will be the topic of the following section.

2.9 Ring Laser Gyroscope RLG

We now have collected the required knowledge for operating a single-mode Helium-Neon ring laser. In this section we shall discuss what happens to the laser modes, when this ring laser is set in rotation.

There are different models to describe the effect of rotation on the ring laser. We shall choose a clear way with the help of the well known Doppler effect. The starting point of the laser oscillations is the spontaneous emission, produced by the excited neon atoms. When such an atom is at rest, it emits the frequency ν_0. If it is moving with velocity v, the emission frequency ν changes due to the Doppler effect to:

$$\nu = \nu_0 \left(1 + \frac{v}{c}\right)$$

If the velocity v arose as a result of the rotation, its value is:

$$v_{rot} = r \cdot \omega$$

where ω is the angular speed and r is the distance of the atom to the centre of rotation. As a result of the rotation, the emissions frequency changes to:

$$\nu_+ = \nu_o \left(1 + \frac{v}{c} + \frac{r \cdot \omega}{c}\right)$$

The above expression applies to atoms, whose velocity v is in the direction of rotation (v_+). The following expression applies to atoms, whose velocity (v_-) is against the direction of rotation:

$$\nu_- = \nu_o \left(1 - \frac{v}{c} - \frac{r \cdot \omega}{c}\right)$$

The difference $\Delta\nu$ of both the frequencies thus becomes:

$$\Delta\nu = \nu_+ - \nu_- = \nu_0 \left(\frac{v}{c} + \frac{2 \cdot r \cdot \omega}{c}\right)$$

The velocity added due to the rotation is

$$\Delta\nu_{rot} = \nu_0 \frac{2 \cdot r \cdot \omega}{c} = \frac{4 \cdot F}{L \cdot \lambda} \cdot \omega \qquad (7)$$

with:

$$F = \pi \cdot r^2 \text{ and } L = 2 \cdot \pi \cdot d,$$

yields the same expression as for the Sagnac effect with passive resonator (eq. (5)).

2.10 Lock-in effect

However, there is one restriction for equation (eq. (7)) for the actual operation of a ring laser gyroscope. Below a certain rate of rotation, no differential frequency occurs i.e. both the modes do not change their frequencies. Such behaviour can only be explained by a coupling of both the modes.

This coupling occurs because parts of the intensity of one mode go into the other. This happens through scattered light that arises at the surfaces of the resonator mirror. Even today, it is not possible to produce laser mirrors that do not show any scattering.

In practice, this leads to an effect, which poses a certain restriction to the working of the laser gyroscope. The scattered light, appearing unavoidably at the mirrors, leads to an "impurity" of the cw mode with few parts of the ccw mode and vice versa. This coupling could be broken, when the rate of rotation of the gyroscope exceeds a certain limit.

In that case, the resonance frequency of the system for both the modes is separated to such an extent, that the laser has to give up the coupling to continue oscillating. This coupling is also called as lock-in effect and the limit, at which this coupling is broken, is called the lock-in limit.

As already mentioned the cause for the lock-in effect is the scattering at the optical surfaces. When the laser beam strikes an optical surface, scattered light always appears in practice spreading in different directions of space depending on the texture of the surface.
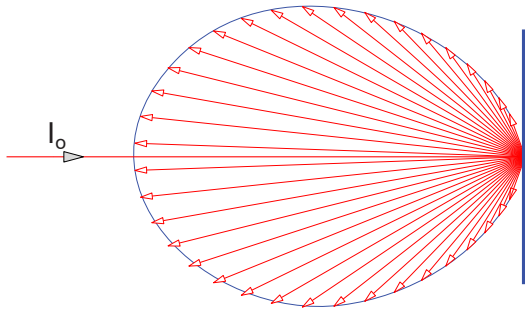

Fig. 31: Light scattering at an optical surface

When a laser beam strikes a reflecting optical surface with the intensity I_0, the reflected ray has an intensity of only

$$I_o \cdot (1 - T - \varepsilon)$$

where T is the transmission and e is the back scattering coefficient. Only that scattered light will have an effect on the laser, which is scattered in the direction of the laser mode (eq. Fig. 31) and has the same phase.

Although the back scattering coefficient is relatively small, it is sufficient to couple both the gyrating modes and produce the lock-in effect.
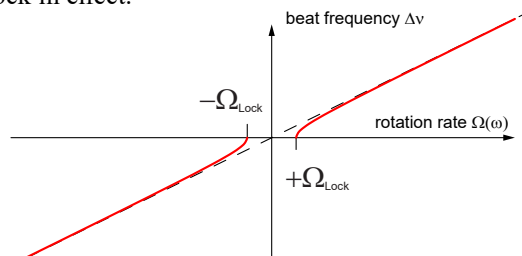

Fig. 32: Lock-in Effect

In principle, the lock-in effect can then be fully eliminated, if one can make the scatter coefficient ε zero. Despite the best polishing and damping, no mirror can be produced today with $\varepsilon = 10^{-7}$. The mathematical description of the lock-in effect is very complex and a complete solution is still not known. Therefore we will be using here the results of the model developed by Fredrick Aronowitz [7]. According to this, there are three areas (also see Fig. 32) for the beat frequency of the ring laser modes:

$$\Delta \nu = \begin{cases} 0 & \Omega \leq \Omega_{Lock} \\ \pm\sqrt{\Omega^2 - \Omega_{Lock}^2} & \Omega \geq \Omega_{Lock} \\ \Omega & \Omega \gg \Omega_{Lock} \end{cases} \qquad (8)$$

where

$$\Omega = \frac{8\pi F}{L\lambda} \cdot \omega$$

and

$$\Omega_{Lock} = A_0 \cdot \frac{c}{L}$$

with A_0 as amplitude of a mode. There is no beat frequency below the threshold Ω_{Lock}. Above it, there is a non-linear relationship and only for higher values of Ω a linear relation. Aronowitz gives the following equation as approximation value for the lock-in threshold:

$$\omega_{Lock} = \frac{c \cdot \lambda}{8\pi F} \cdot \varepsilon \cdot \cos(\beta)$$

In the above expression ε is the back scattering coefficient and β is the phase angle between the back scattered and the resonator wave. Taking the worst case, when β is just 0°, the back-scattering coefficient ε is about 10^{-4} and the leg length of the ring laser is 0.5 m, we get the following value for the lock-in threshold:

$$\omega_{Lock} = \frac{3 \cdot 10^8 \cdot 632 \cdot 10^{-9}}{8 \cdot \pi \cdot 0,25 \cdot \sin(60)} \cdot 10^{-4} \approx 0,2 \ °/s$$

This is a typical value for a good laser gyroscope. One could argue here, that the lock-in effect would put a question mark over the substitution of the mechanical gyroscope by the laser gyroscope. However, this demand is so strong, that one is and always was on the lookout for ways of eliminating the lock-in threshold or at least reducing it to such an extent, that this aim could be fulfilled. The first solution naturally is to let the ring laser rotate at constant speed above the lock-in threshold. However, this reveals the practical difficulty, that the necessary electrical signals and supplies are fed to the system and taken off from it.
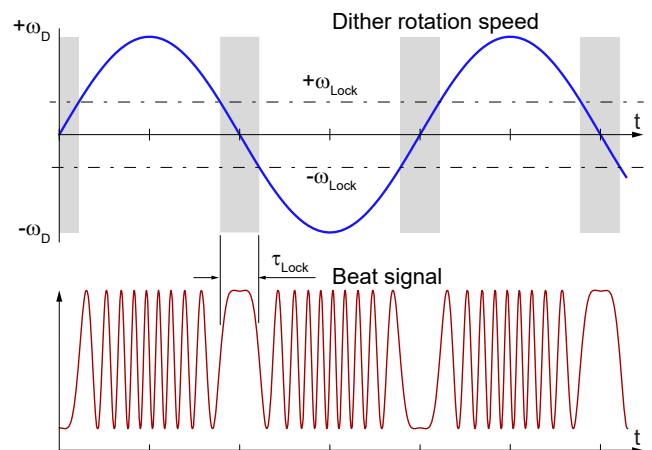

Fig. 33: Dither rotation and beat signal

Worldwide a procedure has been applied, which although does not eliminate the lock-in effect, but certainly reduces its affect on the measurement inaccuracy. For this purpose, the complete ring laser is subject to a periodic oscillation with ω_D (Fig. 33) and with a very small amplitude like a kind of dither.

The upper curve of (Fig. 33) shows the angular dither speed of the ring laser and the lower one, the interference signal. The arrangement ensures that the gyroscope is blocked only within the time τ_{Lock}. Outside this zone, the gyroscope produces a certain number of interference signals in one as well as in the other direction, which together give the result zero. If the whole system now experiences an additional rotation, then this difference is not zero anymore, but instead gives the correct values also for the angular speeds below the lock-in threshold.

The next section deals with the determination and the evaluation of the gyroscope signals.

2.11 Measuring the beat frequency

We expect a frequency difference as per equation (eq. (8)) of the cw and the ccw waves upon rotation of the system in our ring laser. There are two methods for measuring this frequency difference. These method uses the spatial interference as already explained in the Sagnac interferometer, and the other works according to the principle of beam analysis. The advantage of this method is that it is not necessary to combine both the rays by making use of sophisticated devices to produce the required spatial interference.

2.11.1 Interference

Nevertheless, we shall explain the first method, since it is widely used in technical laser gyroscopes. After this, we shall explain the beam analysis method.
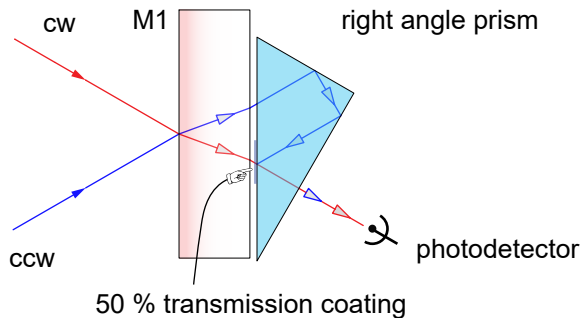
Fig. 34: Reflection prism to combine the cw and the ccw wave

By means of a reflection prism, whose hypotenuse is locally coated with a translucent mirror layer (transmission 50%), the cw and the ccw waves are combined resulting in a spatial interference pattern, whose light and dark transitions are detected with a photodetector. If two detectors are used and placed at a distance of a "half" transition (90° phase-displacement), one can determine the direction in which the gyroscope is rotating.

The beam analysis, as shown in Fig. 35, has less optical effort, but the determination of the direction of rotation is more complicated here.
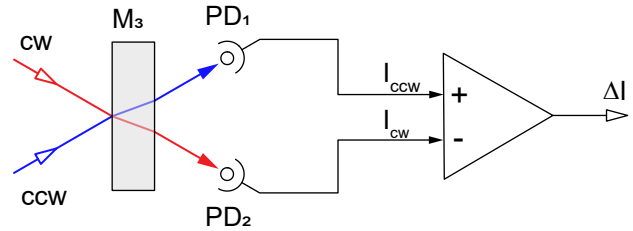
Fig. 35: Beam analysis arrangement

2.11.2 Beam analysis

With this method, the intensity of the cw and the ccw waves is determined with two photodetectors. The beat frequency is measured by subtracting the intensity of both the signals. However, this method only functions, when a certain degree of scattering exists between the cw and the ccw waves. In reality, this is always the case. If the amplitude is Ao in the cw as also in the ccw direction, an additional wave arises due to back-scattering, whose amplitude is $\varepsilon \cdot A_0$, where ε is the back-scattering coefficient. Since, both propagating e.g. in the cw direction, they will superimpose and form a wave with an amplitude of A_{cw}. One finally gets the intensity I_{cw} from the square of the amplitude:

$$A_{cw} = A_0 \cdot \sin(\omega_{cw}t) + \varepsilon A_0 \cdot \sin(\omega_{ccw}t + \beta)$$

$$= A_0 \cdot \left(\sin(\omega_{cw}t) + \varepsilon \sin(\omega_{ccw}t + \beta)\right)$$

$$I_{cw} = \left(A_{cw}\right)^2$$

$$= I_0 \cdot \left(\sin(\omega_{cw}t) + \varepsilon \sin(\omega_{ccw}t + \beta)\right)^2$$

$$= I_0 \left(\begin{array}{l} \sin^2(\omega_{cw}t) + 2\varepsilon \sin(\omega_{cw}t)\sin(\omega_{ccw}t + \beta) \\ +\varepsilon^2 \sin^2(\omega_{ccw}t + \beta) \end{array}\right)$$

The fastest photodetectors of today are in a position to detect frequencies up to $2 \cdot 10^9$ Hz. Therefore, such a detector detects only average values. The sin2 terms oscillate with an essentially higher frequency wcw or wccw, whereby their amplitudes vary periodically between 0 and 1, so that their temporal average value is ½.

$$I_{cw} = \frac{I_0}{2}\left(1 + 4\varepsilon \sin(\omega_{cw}t)\sin(\omega_{ccw}t + \beta) + \varepsilon^2\right)$$

We apply the addition theorem for simplifying the mixed element:

$$2 \cdot \sin\alpha \cdot \sin\beta = \cos(\alpha - \beta) + \cos(\alpha + \beta)$$

The cos term oscillates with the frequency $\omega_{cw} + \omega_{ccw}$ and its amplitude varies between –1 and +1, so that the average value is zero. Thus, we obtain for the intensity I_{cw}:

$$I_{cw} = \frac{I_0}{2}\left(1 + 2\varepsilon \cos\left((\omega_{cw} - \omega_{ccw})t - \beta\right) + \varepsilon^2\right)$$

$$I_{cw} = \frac{I_0}{2}\left(1 + 2\varepsilon \cos(\Delta\omega \cdot t - \beta) + \varepsilon^2\right)$$

Moreover, for the running opposite wave, we get:

$$I_{ccw} = \frac{I_0}{2}\left(1 + 2\varepsilon\cos(\Delta\omega\cdot t + \beta) + \varepsilon^2\right)$$

building the difference $I_{cw} - I_{ccw}$ we get:

$$\Delta I = I_0\cdot\varepsilon\cdot\left(\cos(\Delta\omega\cdot t - \beta) - \cos(\Delta\omega\cdot t + \beta)\right)$$

or:

$$\Delta I = 2\cdot I_0\cdot\varepsilon\cdot\sin(\Delta\omega\cdot t)\cdot\sin(\beta) \qquad (9)$$

In case of the rotation of the ring laser above the lock-in threshold, eq. (9) varies continuously between ΔI and $-\Delta I$ corresponding to:

$$\Delta I = 2\cdot I_0\cdot\varepsilon\cdot\sin(\beta)\begin{cases}1 & \Delta\omega\cdot t = n\cdot\dfrac{\pi}{2} \\[2mm] -1 & \Delta\omega\cdot t = n\cdot\dfrac{3}{2}\pi\end{cases}$$

The maximum difference of the intensities of both the modes thus becomes:

$$\Delta I_{max} = 4\cdot I_0\cdot\varepsilon\cdot\sin(\beta) \qquad (10)$$

One would expect, that this modulation depth would be relatively small because of ε. However, one must consider that the scattered wave is also amplified in the ring laser and thus, shows much better signal strength as expected by eq. (10). In reality one gets about 30 – 40% modulation, this can be increased with subsequent amplifying stages. Unfortunately, this method of beam analysis does not provide any information about the direction of rotation of the ring laser. This must be done by detecting the appearance of the lock-in area during the dither movement, because the direction of rotation changes precisely in this area. This could become problematic due to errors appearing in this area because of disturbances. Therefore, this procedure can be used properly only when the complete system is closed and actively stabilized. In an early developmental phase we checked in detail this method at an open system, like the one being used here, and then rejected it, since an experimental system with a lot of freedom of adjustment does not possess a fixed working point as demanded by this method. To justify the widest possible range of possible working points, we have realized a special interference assembly, which comes very close to these requirements: a push-pull interference assembly as shown in eq. Fig. 36.
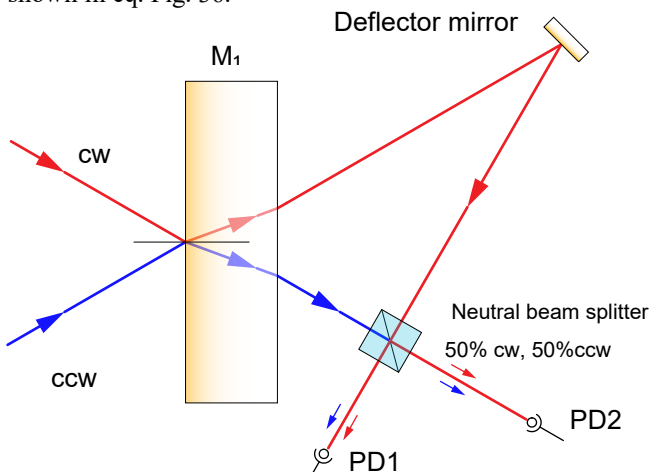
Fig. 36: Push-pull interference formation

In this arrangement, the neutral beam splitter divides the in-

tensity of the CCW mode in two equally large portions. The CW mode is deflected with a mirror in such a way, that the beams overlap with those of the CCW modes and interfere. The interference pattern detected by the photodetector PD1 has a phase shift of 180° compared to that of PD2 (Fig. 37).
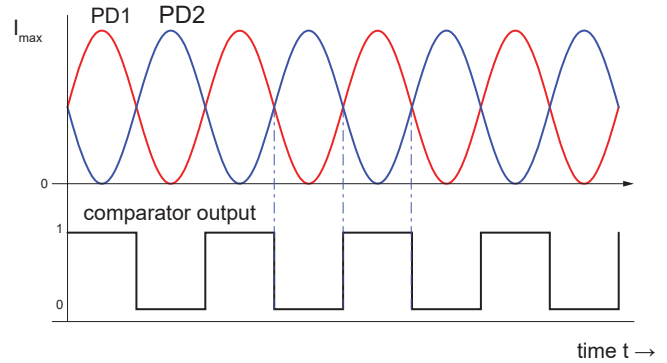
Fig. 37: Ideal contrast

Fig. 37 shows the output signals of the photodetectors PD1 and PD2 for the unrealistic case with 100% interference contrast. The comparator switches from logical zero to logical one or from logical one to zero exactly when both the signals possess the same amplitude.

We shall now consider a more realistic case (Fig. 38), in which the contrast is clearly less. The advantage of using signals shifted in phase by 180° can be seen clearly here: the output signal of the comparator is independent of the interference contrast and offset variations in a large range.
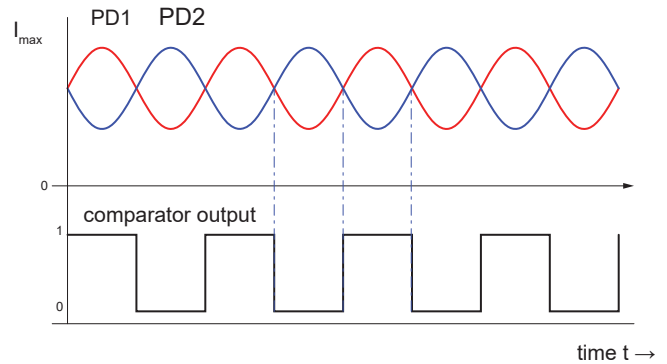
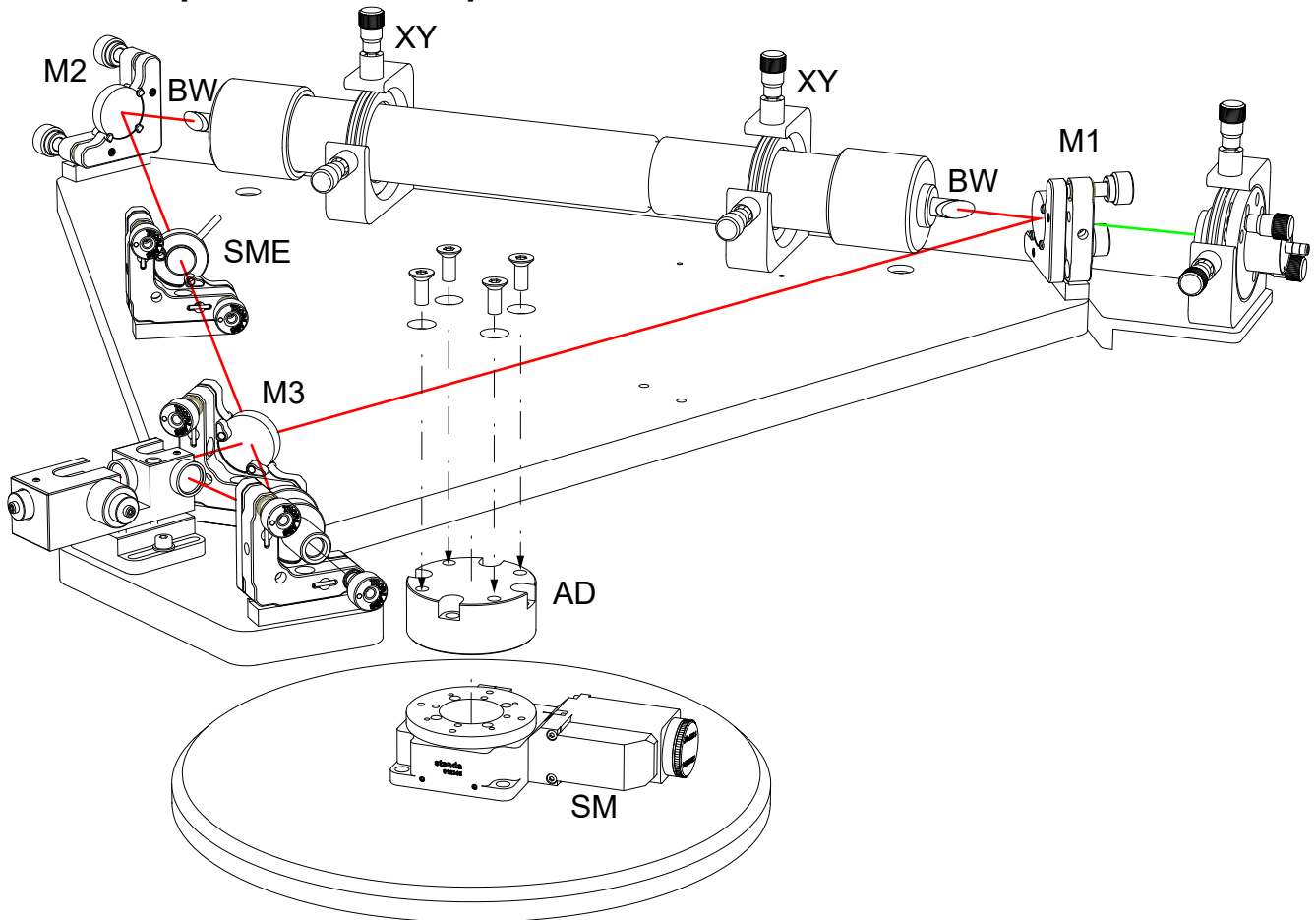**Fig. 38: Real contrast**

3.0 Description of the components

Fig. 39: System Overview

3.1 System Overview

The Helium Neon laser tube is equipped with two Brewster windows (BW) and is mounted into a pair of XY adjusters (XY). The tube is fixed by slightly pressed soft rubber O-rings. The precise adjustment screws allow the tube to be aligned in XY direction. The interplay of both adjusters also allows the angular wobble of the tube. For the operation, a high voltage power supply is supplied (DC-0064, page 22) which provides the start-up ignition voltage of about 10 kV and 6.5 mA at 1400 V for continuous operation.

The sturdy and yet lightweight ribbed aluminium plate has an equilateral shape. On each corner an adjustable laser mirror holder is mounted forming with mirror M1, M2 and M3 the optical cavity. The plate is attached to the drive unit with an adapter (AD) with four countersink screws and will be dismounted from the drive unit before shipment. Although it is not really a circle such a cavity is also considered as ring cavity. The distance between the mirrors is 460 mm resulting in a cavity length L of 1380 mm and free spectral range ($\delta v=c/L$) of 217 MHz.

The stepper-motor (SM) drives a zero-play pre-loaded worm gear drive which rotates the turntable. The powerful stepper-motor needs 200 full steps per turn which relates to a rotation of 2° or 0.6' per step. The stepper-motor is connected via a 15 pin Sub-D connector to the DC-0300 stepper motor controller (page 18).

3.2 Single mode etalon

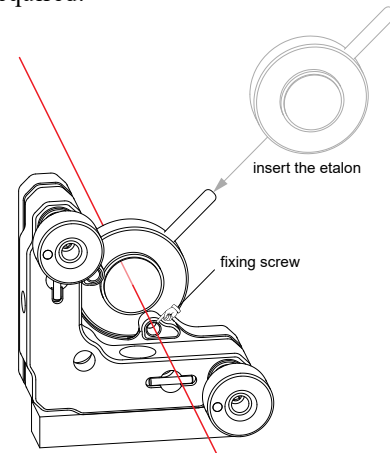To achieve a clean beat frequency, the single mode etalon (SME) is required.

Fig. 40: Single mode etalon it its adjustment holder

For the operation of the laser gyroscope it is required that the laser operates in a single mode only. This is achieved by inserting an etalon into the cavity. A kinematic adjustment holder allows the precise orientation of the etalon with respect to the laser beam.

A quartz etalon with a length of 10 mm is used. The end surfaces are polished very precisely for a parallelism of better than 10 arc seconds. An extra coating is not necessary, since already the Fresnel reflection of approx. 4% per side provides a sufficient finesse. The etalon is mounted into in a 25.4 mm holder with a handle which is kept in place in the adjusting holder.

3.3 Dual beat frequency detector
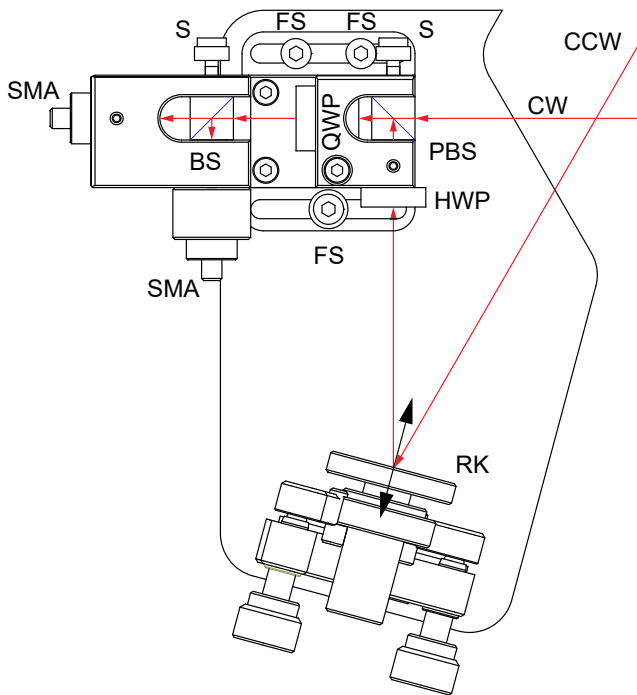
To obtain the beat frequency, the cw (clockwise) and the ccw (counter clockwise) modes must propagate collinear. At mirror M3 a small fraction of both modes is leaving the cavity. The cw mode passes directly the polarising beam splitter (PBS) and the ccw mode is reflected by the mirror M4 in such a way, that it enters the polarising beam splitter (PBS). Since it has the same polarisation as the ccw mode we need to turn its polarisation by 90° so that the mode is reflected inside the PBS and continues to travel collinear with the cw mode. Now, both modes are perpendicularly polarised to each other. The quarter waveplate (QWP) converts both modes into circular polarised light. By using a neutral beam splitter (BS) with a splitting ratio of 1:1 we create two channels. At the end of each channel a polarizer (P1, P2) is located in front of the fibre SMA adapter converting the light back to linear polarisation allowing the detection of the beat frequency. To obtain a 90° phase shifted optical signal the polariser P1 and P2 are oriented under an angle of 45° to each other. This allows the detection of the rotation direction of the laser gyroscope. Each SMA adapter is connected via a plastic optical fibre to the 2 channel photodiode amplifier DC-0080 (page 20).

3.4 Green adjustment laser
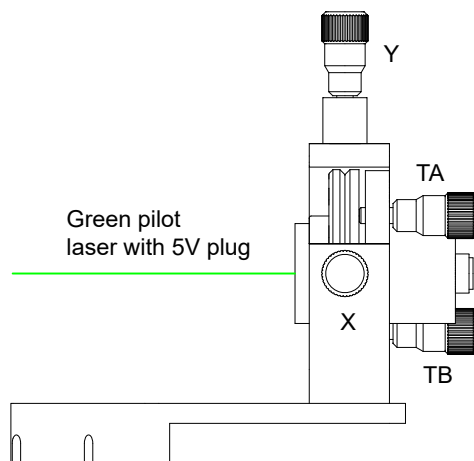
For the reliable alignment of the mirror of the laser ring cavity, a green emitting laser pointer is used. It is held in a four axes adjustment holder in such a way that the pilot laser can be shifted and tilted to align the alignment beam with respect to the laser tube via the mirror M2.

This module is designed as an attachment to OM-0700 Gyroscope turn table and provides a green emitting DPSSL which is mounted into a 4 axes kinematic mount. It is used for the initial alignment of the HeNe tube as well the three ring laser mirror of the laser gyroscope. Four precise fine pitch screws of repetitious accuracy allowing the translative (X,Y) and azimuthal (TA, TB) adjustment. The alignment laser is powered by 5V USB wall plug power supply.

3.5 DC-0100 Stepper motor controller

This device controls two phase stepper-motors with a maximum current of 1 A. The stepper-motor is connected via a 15 pin SubD HD connector located at the rear of the device. The controller is operated with a microprocessor and a touch screen is used to select the parameter to be changed. A digital knob is used to set the value for the selected parameter. The controller is used for rotation as well as translation stages and the corresponding user interface is selected at the start-up of the device. A USB bus is provided to control and collect data with external software.

Experimental Setup

The backside of the controller provides the 12VDC power connector and main switch. A USB bus is provided for external programming. The stepper-motor is connected via the 15 pin HD SubD connector.

Start page

After switching the device on with the main switch on the backside, the start screen appears and shows the model of the device. Touching the screen opens the main page.
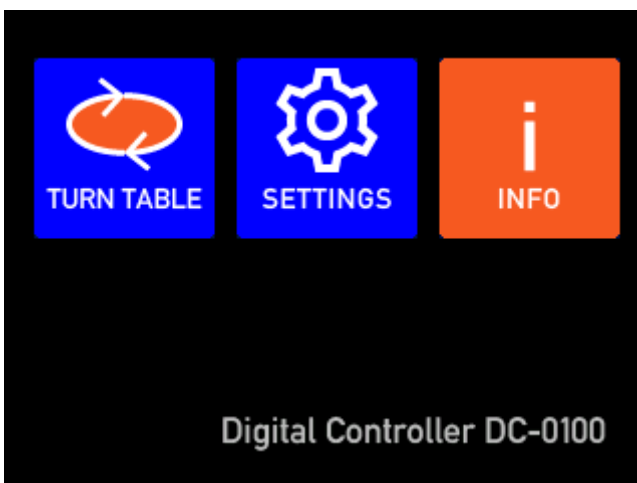
Main Page

After touching the start page, the Main Page shows up with three touch buttons. The "TURN TABLE" button opens the turn table screen for direct access to the turn table rotation. The "SETTINGS" button opens the screen for the pre-sets of the cycling motion. The "INFO" shows general information.
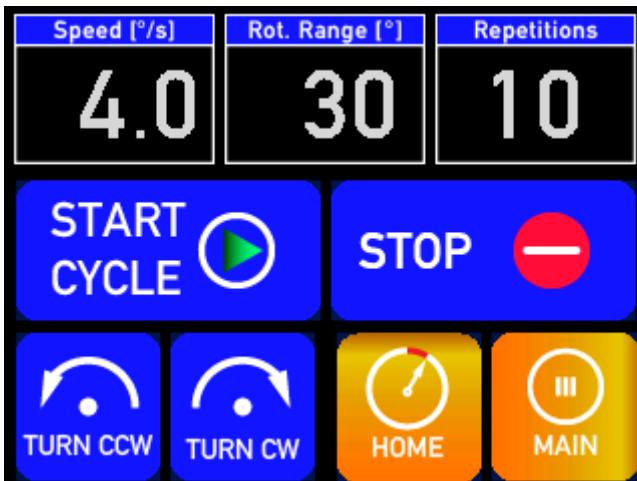
Settings Page

When touching a number field, it will be highlighted and becomes active. The desired value is set by turning the knob. The speed can be set from 0.1 - 12 °/s, the rotation range up to 180° and the repetition rate up to 99. Touching "TURN CCW or CW" lets the table turn accordingly with the selected speed. Touching the "START CYCLE" button, the cycle starts and shows the turn table screen. The "STOP" buttons ends the manual turning. The "HOME" button switches to the turn table screen and the "MAIN" button to the main screen

Experimental Setup

Turn table screen

The gauge shows the position of the turntable. A desired position is approached by touching the turn CW or CCW button and set to the actual zero position. Touching the gauge brings the settings page back.
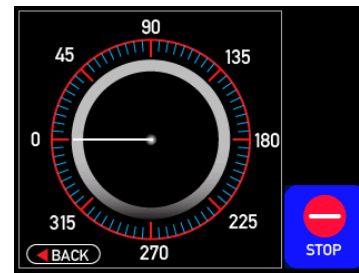
When, either the CW or CCW button has been touched, both buttons disappear and only the "STOP" button comes up. After touching the stop button, the motion stops and the CW and CCW button become visible again.
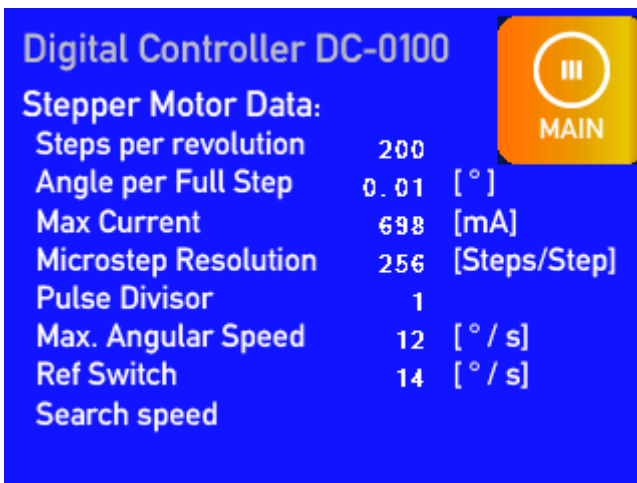
Info Screen

The screen shows general information about the stepper-motor and the maximum angular speed, which is limited by the software.

Emergency Button

The central knob for setting the device parameter provides a switch, which is activated by pressing down the knob. All motions will be stopped immediately and the emergency button scree is shown.


3.6 DC-0080 Quad counter & 2 channel photodiode amplifier

The device serves as 2 channel photodiode pre-amplifier and as quadrature counter. The gain, offset and switching threshold independently be set for each channel with the touch panel and digital knob. The output of each pre-amplifier is available via 4 BNC panel jacks at the rear of the device. From the two analogue signals the TTL quadrature signals are formed and counted by the quadrature counter. The signal of the counter is available as TTL signal at two BNC panel jacks at the rear of the device. The controller is equipped with a touch panel display and with the digital knob, the parameter like photodetector gain, offset and counter threshold are selected and applied.

Experimental Setup

Fig. 41: Rear panel of the DC-0080 controller
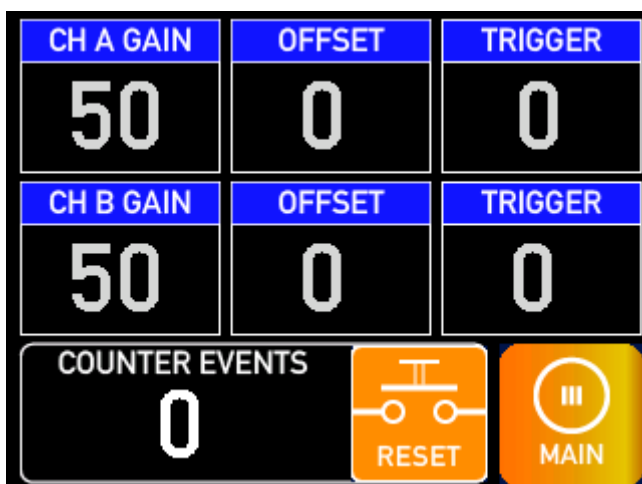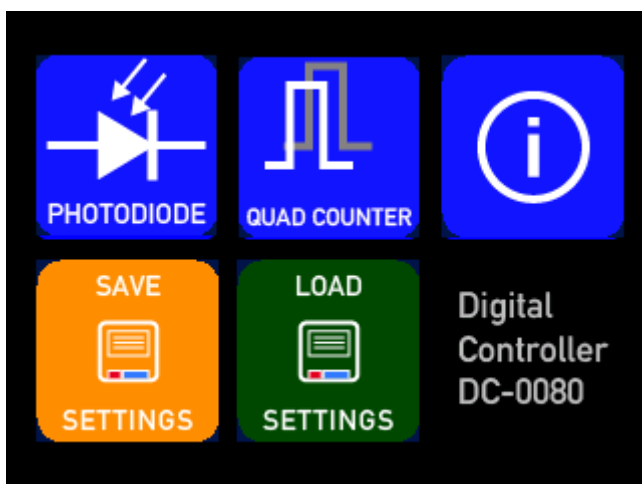
The backside shows the 12V DC socket and the main switch. A USB bus is provided for programming. The two plastic optical fibres from the beat frequency detection unit are screwed to the SMA sockets which contain two fast photodiodes. This arrangement has the advantage, that the sensitive photodiodes are protected against environmental irradiation. Each channel has an analogue and digital output to monitor the photodetector signal on an oscilloscope.

Start page

After switching the device on with the main switch located at the rear panel, the start screen appears and shows the model of the device. Touching the screen opens the main page.

Main Page

The main page shows touch buttons to go to the photodiode pre-amplifier settings, the settings and readings of the quadrature signal counter. The settings can be stored in the non volatile memory of the controller. Touching the "LOAD SETTINGS" loads these settings into the working memory. Further information is displayed by touching the info button.
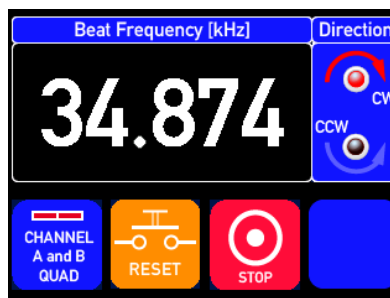
Photodiode Pre-amplifier Settings

The DC-0080 is a two channel amplifier. For each channel the gain, offset and trigger level for the TTL comparator can be adjusted. When touching a number field, it will be highlighted and becomes active. The desired value is set by turning the knob. The settings shall be modified while monitoring the analogue as well as digital signal with an oscilloscope. Once the settings are optimised, the rectangular signal appears and the counter starts. The counted events are set to zero by touching the reset button.
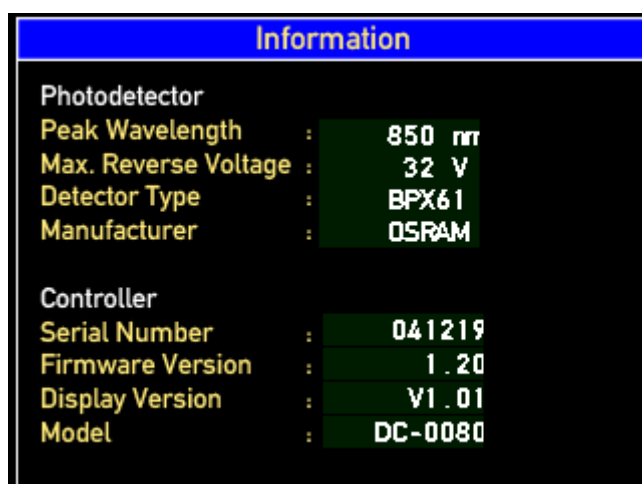
Counter Page

The beat frequency can be measured in two ways, either by using the quadrature signal or by using the signal of channel A only. The mode is toggled by touching the "CHANNEL A ONLY" button. In the quadrature mode a direction indicator becomes visible. In both cases the counter starts by touching the "START" button and stops by touching the "STOP" button. If the counter is active, changing to the main page is not possible.

Info Page

On this page information about the photodetector and the controller itself are given.

3.7 DC-0064 High voltage supply 6.5 mA

This device is used to operate a HeNe laser with a fixed discharge current of 6.5 mA. The HeNe laser is connected to the high voltage BNC jack. A safety key switch prevents the unauthorised operation. The device comes with a 100/230 VAC / 12 VDC wall plug power supply.

Experimental Setup

4.0 Ring laser initial alignment

4.1 Threading the pilot laser through the capillary
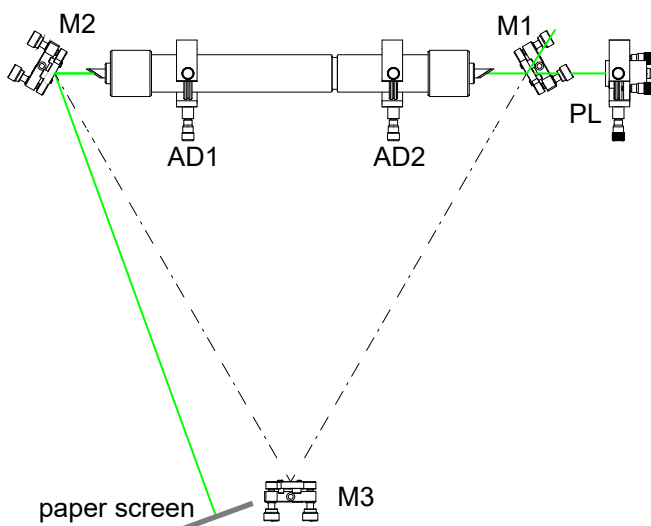
The HeNe laser tube is centred in its adjustment holder AD1 and AD2 by sight. The pilot laser is connected to its 5VDC supply. The green beam of the pilot laser passes the mirror M1. Align the beam so that the beam enters the first Brewster window. Align the mirror M2 in such a way, that the green beam can be observed on a sheet of white paper.
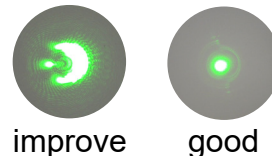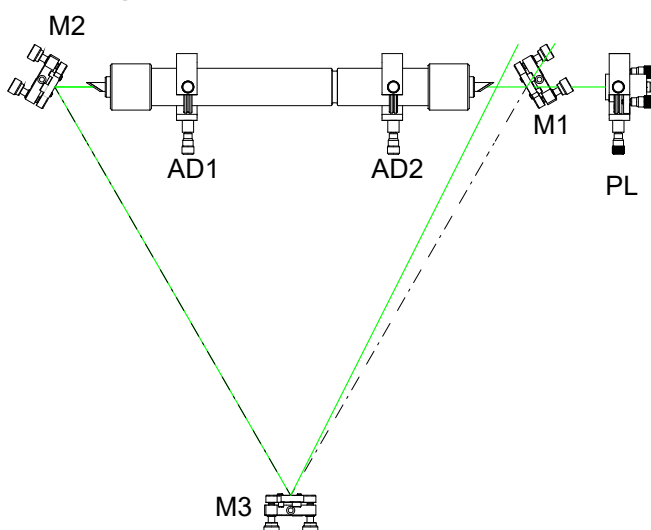
improve   good

Now, align the XY and TA and TB screws alternately and observe the spot on the paper. The goal is to thread the beam through the capillary without hitting it inside. After a while a "good spot" is obtained. The fine tuning can be accomplished by adjusting the laser tube with AD1 and AD2.

4.2 Align mirror 2 to mirror 3

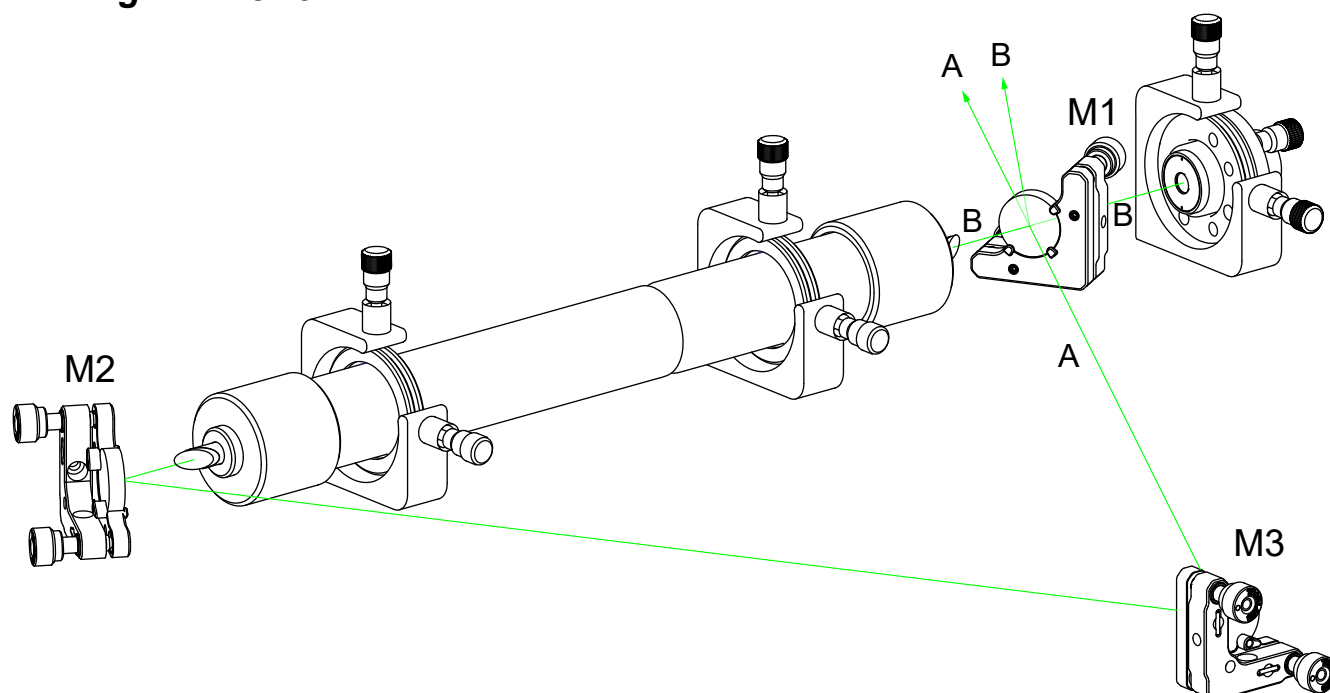In this step the beam which is reflected by the mirror M2 is adjusted so that it hits the mirror M3 in its centre.

4.3 Align mirror 3 to mirror 1
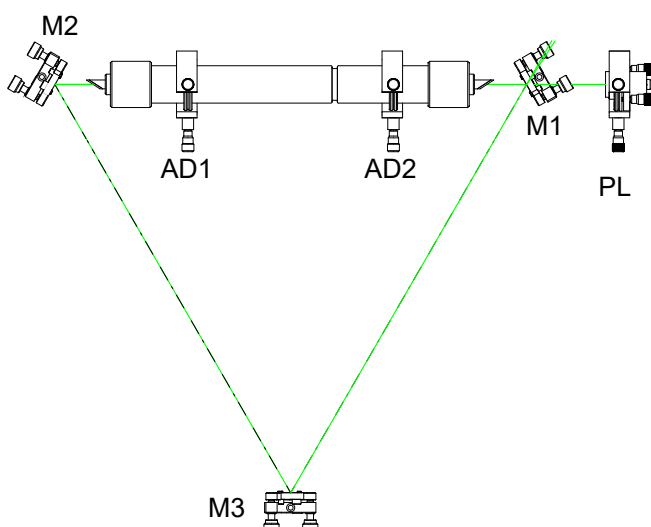
The mirror M3 is adjusted in such a way, that the beam hits the mirror M1 exactly the spot of the transmitted beam from the pilot laser (see also next step).

Experimental Setup

4.4 Align mirror 3

The beam B is transmitted by mirror M1 and enters the Brewster Window. However, a significant amount is reflected at the back of the mirror coating of M1. In the previous step we aligned the beam A to the centre of the spot of the beam B on the mirror M1. The beam A is reflected, but also transmitted from mirror M1. In the last alignment step the mirror M1 needs to be aligned. For this, we observe the spots of A and B in a distance of 1 or 2 metre on a wall for instance. The goal is now to align only M1 in such a way, that the spot of beam B hits the spot of A. Switch on the high voltage supply of the laser tube and the ring laser should work.

4.5 The ring laser is running
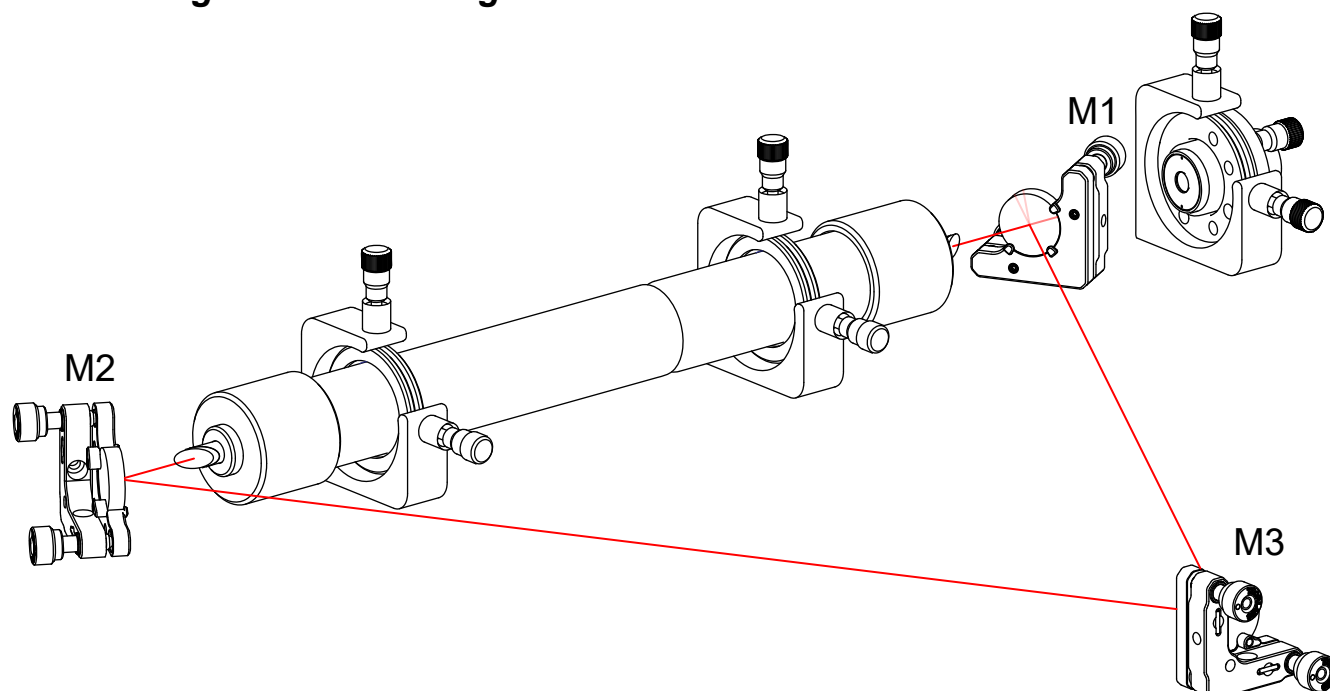
Hurrah, the ring laser is working. Realign all adjuster for best performance.

Experimental Setup

4.6 Insert the etalon


insert the etalon

fixing screw
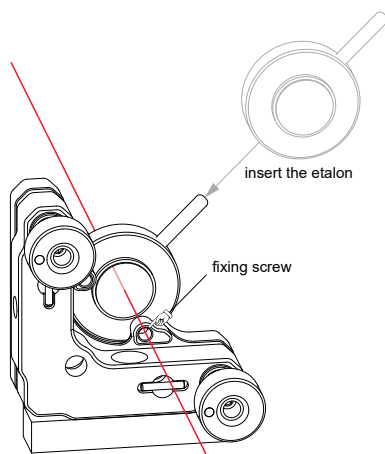
The adjustment holder for the etalon is already mounted to the turn table. During the initial alignment, the etalon is removed from its holder. After successful laser alignment the etalon is inserted into its mount and fixed by the clamping screw. It may happen that the laser stops working. In this case try to align the etalon to get the laser operation back. If it does not work, switch on the pilot laser again and align the etalon perpendicular to the green beam. This will bring back the HeNe laser oscillation.

4.7 Single mode operation

M2

Etalon

M3

M1
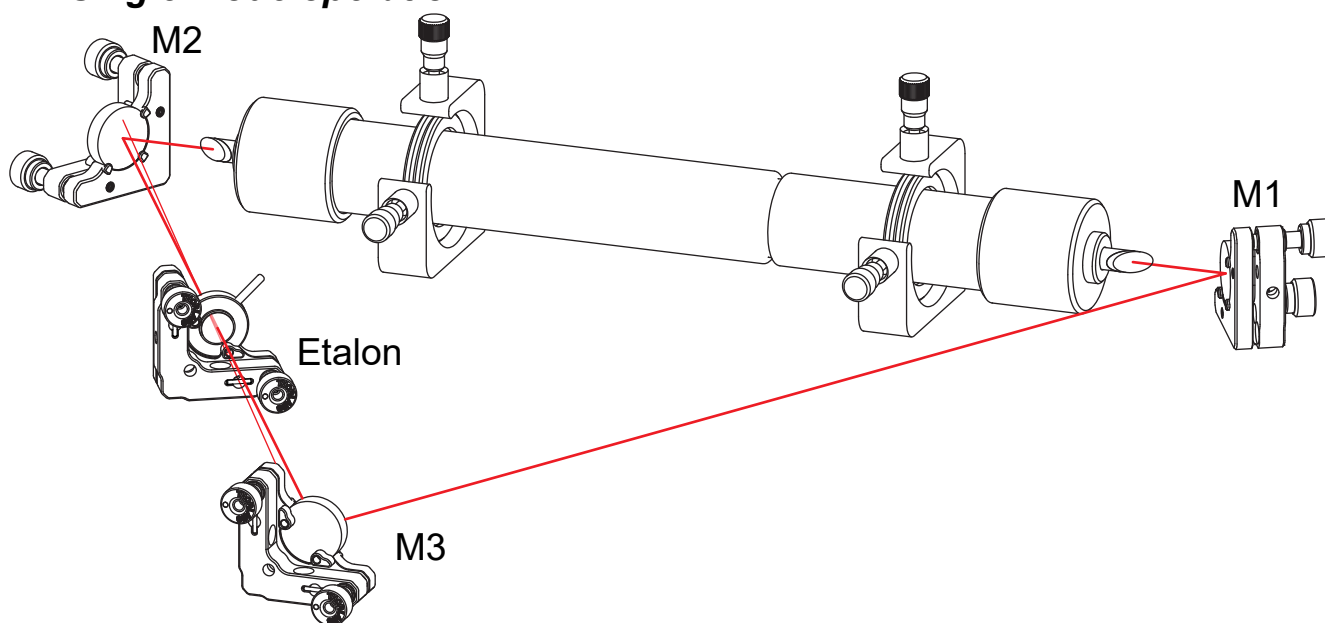
If the etalon is aligned perpendicular to the laser beam, it operates in the zero order. When the etalon is tilted, the laser oscillation may stop and come back. It is now in the first order and a reflected beam appears on the mirror M2. In the zero order still multimode oscillation occurs, while in the zero or even higher order only one mode oscillates.

Experimental Setup

## 4.8 Alignment of the beat frequency detector
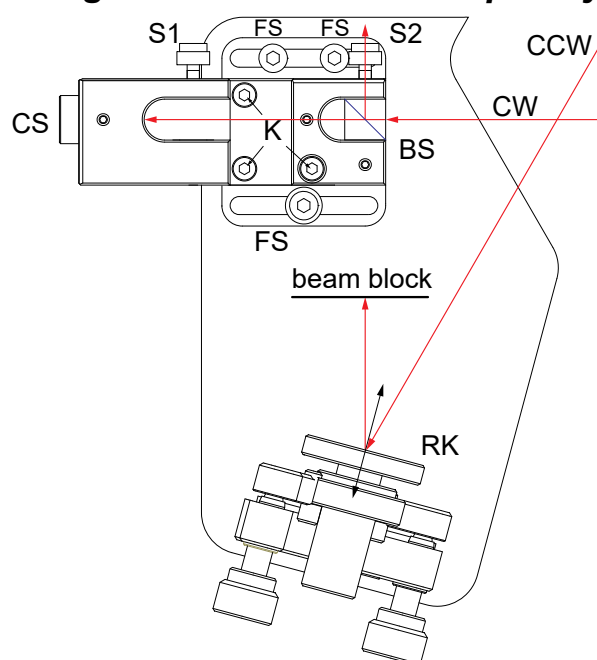
4.8.1 One detector arrangement

For the beginning, it may make sense to use the simple "one detector" arrangement. For this purpose the neutral beam splitter (BS) is carefully inserted and fixed with the nylon set screw S2. Block the ccw beam with a piece of paper. To make sure, that the cw laser beam leaves the detection unit coaxial, we plug the white screen (CS) into the detector holder. Now we can watch the spot of the cw laser beam on the small white screen and determine if it is centred. If not, loosen the FS screws for sidewise adjustment. With the K screws the carrier is tilted up and down.

White screen (CS)
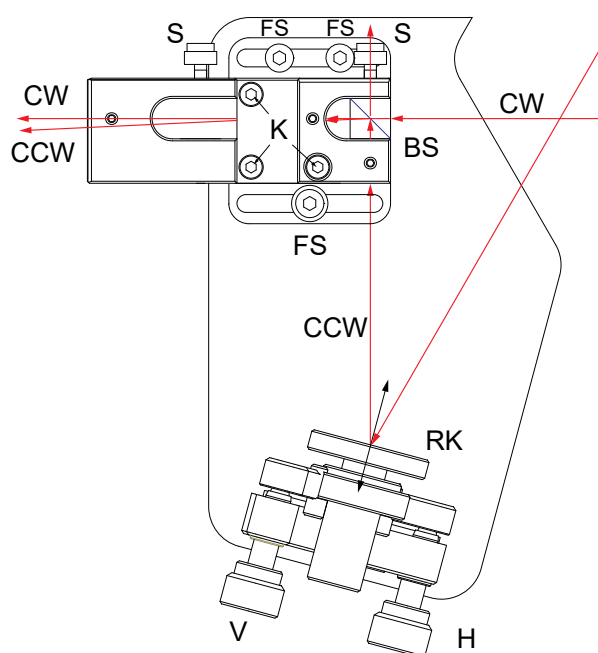
4.8.2 Align for best contrast

Ones the assembly has been aligned for the cw beam, we remove the sheet of paper which was blocking the ccw beam. Align the V and H screws to direct the beam to the centre of the beam splitter BS. The ccw beam also appears beside the cw beam at the exit of the assembly.

It is the gaol to align the ccw beam such, that it is propagating coaxial with the cw beam. For this purpose the locations of the cw and ccw spot is observed on a screen (wall) about 2 metre apart and with a piece of paper 5 cm behind the beam outlet. Both spots must centrically overlap. If not, align the V and H screws the overlap in the farer distance and with the mirror RK in the near distance. Turning the mirror shifts the ccw beam right or left. The alternating adjustment in the far and near distance converges sooner or later. With a simple lens, the coaxial propagating beams can be expanded showing a static interference pattern when the ring laser is not rotating.

Now the set-up is ready for measurements without direction discrimination.

Once the interference adjustment has been finished, the fibre adapter is inserted into the assembly and fixed with the set screw. Next, the plastic optical fibre is inserted and screwed to the adapter. The other end of the fibre is attached to DC-0080 (see "Fig. 40: Single mode etalon it its adjustment holder" on page 17).
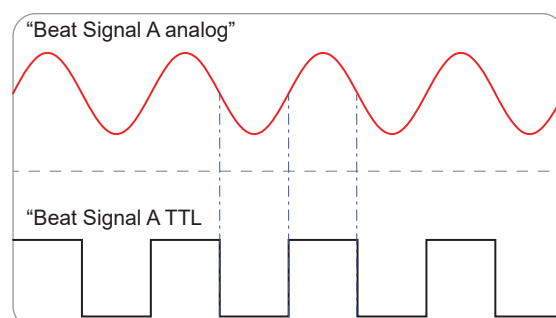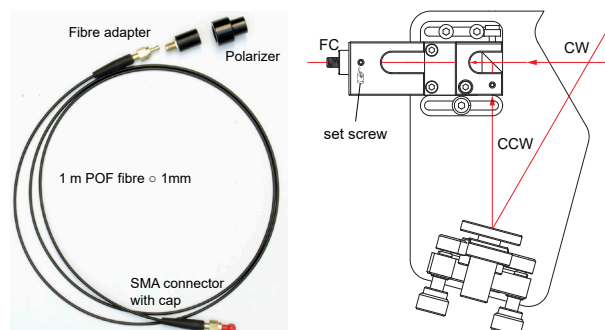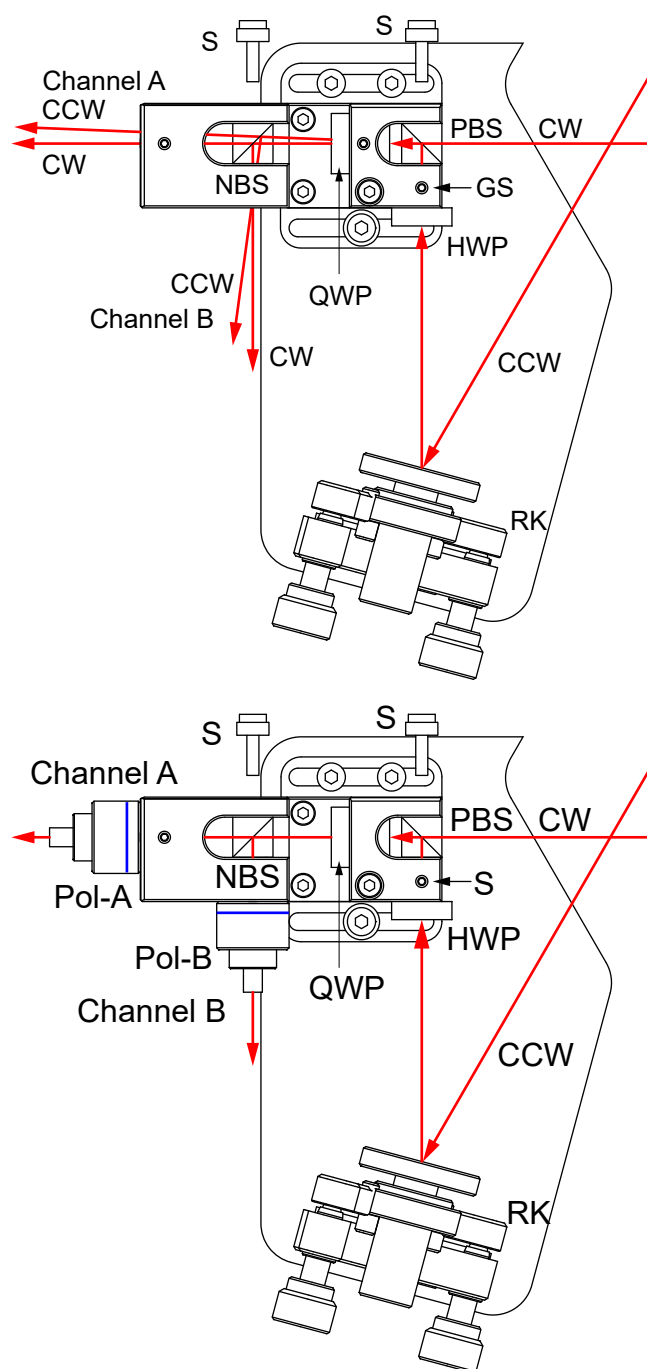

Experimental Setup

Fig. 42: Oscilloscope image of a good aligned assembly

4.9 Dual detector set-up

This set-up is used, when the electronic direction recognition is applied. Instead of the neutral beam splitter a polarising one (PBS) is used. The PBS is placed in such a way, that its centre is in line with the fixing grub screw (GS). With the nylon screw (S) it is fixed in its position. Next, the half wave plate (HWP) is placed into position. It is rotated, so that the observed intensity leaving in channel A direction becomes maximal. In this position it is fixed with the grub screw (GS). The neutral beam splitter cube is inserted and fixed with the nylon screw (S). Now, the quarter wave plate (QWP) is inserted and slightly fixed. It shall be set under 45° with respect to the cw or ccw beam which is checked ones beat frequency signals available and visible on the oscilloscope. For this purpose, the QWP is rotated to achieve the maximum contrast of the signal.

Finally, the polariser A and B are plugged to the assembly. In addition, both optical fibres are connected.
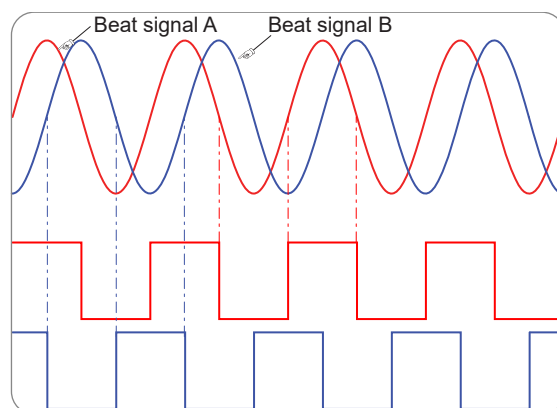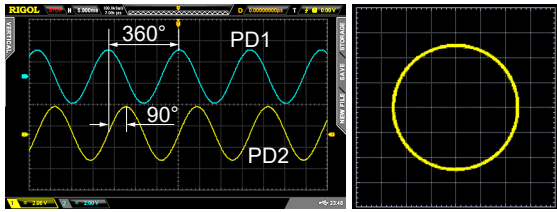

Fig. 43: Phase shifted beat signals

The phase shift between the beat signal A and B depends on the relative angle of the polariser, which can be set by rotating one of them.

Experimental Setup

5.0 Measurements

5.1 Beat frequency signals 90° phase shift and XY representation

Once the initial alignment of the ring cavity has been completed and the ring laser operates with the inserted etalon, it is time to adjust the beat frequency detector. PD1 and PD2 are connected to the photodiode amplifier and the output connected to an oscilloscope. By aligning the polariser P1 and P2 the phase shift of 90° between the signal of PD1 and PD2 is achieved. In case both amplitudes are the same a circle appears when the oscilloscope is switched to the XY mode. If the gyroscope is resting, only a dot on the circumference track is visible. Depending of the rotation direction, this dot moves accordingly.

5.2 Beat frequency converted to TTL and its XY representation
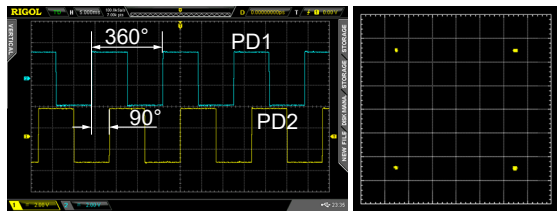
The DC-0080 amplifies not only the photodiode signal, it also converts it to TTL level. In the XY representation we will notice a dot jumping from one corner to the next one. Depending on the rotation of the laser gyroscope this dot either jumps in the cw or ccw direction. The TTL signal of PD1 and PD2 is connected to the input of a quadrature counter which fulfils three tasks. Firstly it interprets the rotation direction, secondly it counts the TTL events and thirdly it can interpolate one event into 4 (each dot of the corner). In frequency mode the beat frequency is measured and displayed.
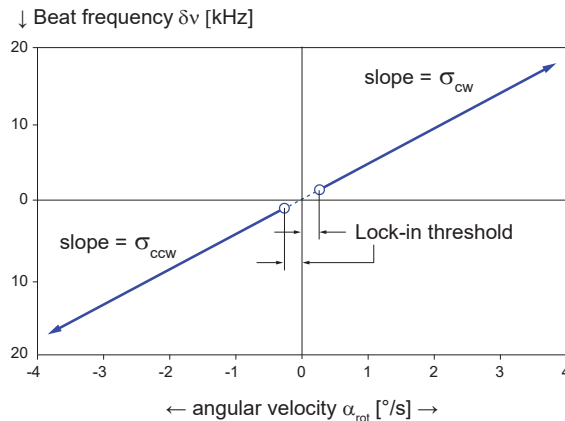
5.3 Measure the beat frequency versus rotation speed

Fig. 44: Lock-in threshold and gyroscope constant

$$\delta \nu_{beat} = \frac{4 \cdot F}{L \cdot \lambda} \cdot \omega_{rot}$$

This formula derived from Sagnac's equations describes the dependency of the beat frequency on the rotary frequency ω_{rot} and constant parameter of the gyroscope. F denotes the area which is encompassed by the light beam, L is its circumference and λ the wavelength of the laser. Applying this formula to our gyroscope with the equilateral shape with the length a of one side of 460 mm we get

$$\delta \nu_{beat} = 4.202 \cdot 10^5 \cdot \omega_{rot}$$

Converting ω_{ro} into the angular velocity α_{rot} in °/s we get:

$$\delta \nu_{beat} = 7.334 \cdot 10^3 \cdot \alpha_{rot}$$

With an angular speed of 1°/s for example, we should expect a beat frequency of 7.334 kHz.

It is a part of the measurement task to determine this value. The stepper-motor controller is set in such a way, that the gyroscope shall turn let's say 180 ° in cw and subsequently in ccw direction for a given set of angular velocities α_{rot}.

A sample graph with arbitrary units is shown in Fig. 44. From the slope of the cw and ccw rotation we will get the value of σ and compare it with the predicted value. Furthermore the lock-in threshold is determined.

Bibliography

1.   UM-LM03 Manual Fabry Perot Resonator

2.   Michelson, A. A.; Gale, Henry G. (1925). "The Effect of the Earth's Rotation on the Velocity of Light, II". Astrophysical Journal. 61: 140

3.   Rosenthal, A.H. (1962). "Regenerative Circulatory Multiple-Beam Interferometry for the Study of Light-Propagation Effects". J. Opt. Soc. Am. 52 (10): 1143–7. doi:10.1364/JOSA.52.001143

4.   Macek, W.M.; Davis Jr., D.T.M. (1963). "Rotation rate sensing with travelling-wave ring laser". Appl. Phys. Lett. 2 (3): 67–68.

5.   BLAZING GYROS - THE EVOLUTION OF STRAPDOWN INERTIAL NAVIGATION TECHNOLOGY FOR AIRCRAFT, Paul G. Savage, Strapdown Associates, Inc. (SAI)

6.   H. Kogelnik and T. Li. "Laser Beams and Resonators" Vol. 5, Issue 10, pp. 1550-1567 (1966)

7.   Fredrick Aronowitz, The Laser Gyro in "Laser Application" Vol. 1, p. 134, Academic Press 1971).